At position −93 from the transcription start site of mPSP94 gene, there is an ARE-like sequence, TACCTAnnnTGTTCT that contains half site of consensus ARE, TGTTCT. We demonstrated that this site is indeed a functional ARE for androgen-dependent transcription in the present study. Interestingly, the promoter region also contains sequences similar to estrogen responsive element (ERE) which enhance androgen-dependent promoter activity of the gene in the presence of the estrogen receptor (ER) α.

2. Materials and methods

2.1. Construction of reporter plasmids and transient transfection

The 5′f region of the mPSP94 gene (GenBank AF087140) was cloned by precise PCR. Specific primers at positions −1202 and +21 from the transcription start site were designed (5′-AGCAACCTCACTTGTTCCTCAGA and 5′-GGTACCTCCAGCAAAGTCCTTG). PCR was performed with PrimStar Taq (Takara Bio., Otsu, Japan) and genomic DNA of C57BL mouse liver following the manufacturer's recommended conditions. After adding an adenosine residue, the PCR fragment was cloned into the pCR2.1-TOPO TA cloning vector (Invitrogen, Carlsbad, CA, U.S.A.) and the sequence confirmed with a capillary sequencer, ABI PRISM 310 (Applied Biosystems, Foster City, CA, U.S.A.). Truncated fragments of the 5′f region were also prepared by PCR with LA-Taq (Takara Bio.) between positions −450, −358, −200, −118, −95, −76 and +21 from the cloned 5′f region −1202/+21. Each fragment was cloned into the PCR2.1-TOPO vector. Sac I/Xho I-digested fragments were then inserted into the corresponding restriction enzyme sites of the pGL3-basic luciferase reporter plasmid (Promega, Madison, WI, U.S.A.), and designated as mPSP94p-1202, -450, -358, -200, -118, -95, -76.

Mutations and deletions were introduced into pGL3 promoters using a QuickChange Site-Directed Mutagenesis Kit (Agilent Technology, Santa Clara, CA, U.S.A.). For ARE analysis, nucleotides between positions −85 and −79, and between −44 and −31 were deleted from mPSP94p-118. In addition, the TGT sequence at position −84 was changed to GAG. For ERE analysis, estrogen responsive element (ERE)-like sequences between positions −435/−421 and −216/−202 were deleted from the PSP94p-450 reporter. Construction of the hAR and hER expression plasmids, pSG5-hAR, pSG5-hERα, pSG5-hERβ were as described previously [17]. PhRL-CMV (Promega) was utilized as an internal control.

CHO cells were plated at a concentration of 2×10^4/well in 48-well plates and transiently transfected with 300 ng of a reporter, 30 ng of pSG5-hAR and 2 ng of phRL-CMV with Hilymax transfection reagent containing a synthetic cationic lipid (Dojindo Laboratories, Kumamoto, Japan), following the manufacturer's protocol. The weight ratio of the reagent to DNA was 1:1. After 24 h of incubation, cells were harvested with 25 μl of cell lysis buffer (Promega) and firefly and renilla luciferase activities determined with a Dual Luciferase Assay Kit (Promega) by measuring luminescence with a Lumino/Fluro meter. Firefly luciferase reporter activity was normalized to renilla luciferase activity from phRL-CMV. For transfection into the LNCaP cell line, a concentration of 4×10^4 cells was plated into 48-well plates; the ratio of reagent to DNA was 3:1.

DNA motif searches for ARE and ERE were performed using TRANSFAC at http://www.genome.jp/tools/motif/.

2.2. Cell culture

The CHO cell line was maintained in DME medium (Sigma Chemical Co., St. Louis, Mo., U.S.A.) containing penicillin and streptomycin with 5% FBS (Biosolutions Japan Co., Osaka, Japan). The LNCaP cell line was maintained in RPMI-1640 medium (Sigma Chemical Co.) with 10% FBS and penicillin/streptomycin. For hormone treatment experiments, cells were maintained for a week in phenol red-free medium (Sigma Chemicals) containing the same antibiotics along with dextran-charcoal treated sera. Dihydrotestosterone (DHT), hydroxy flutamide (OH-flutamide), 17β-estradil (E_2) and ICI182780 were purchased from Wakojunyaku K.K., Osaka, Japan, Toronto Research Chemicals Inc., North York, ON, Canada, Sigma Chemicals and Tocris Bioscience, Ellisville, MI, U.S.A., respectively.

3. Results

3.1. DHT-dependent promoter activity of the 5′f region of mPSP94 gene

Data concerning promoter activity of the cloned 5′f region −1202/+21 and the successive truncated regions in response to DHT are summarized in Fig. 1A. Position numbers are assigned based upon the transcription start site (+1). Significant induction of luciferase activity by DHT was noted in all constructs but mPSP94p-76, which suggested that the region between positions −95 and −76 was essential for androgen-dependent transcription. The induction appeared lower with reporter constructs containing longer distal 5′f regions of the promoter, although these remained significant in terms of induction.

Since there is a half conserved ARE sequence between positions −84 and −79, luciferase activities of the mPSP94p-118 reporter deleting this region and a reporter exhibiting mutations within this site converting TGT to GAG at position −84 were examined and are shown in Fig. 1B. Those constructs disrupting the half ARE site showed no induction of luciferase activity in response to DHT, while a reporter constructing deleting elsewhere (Δ-44/-31) exhibited DHT-dependent transcription.

Induction of mPSP94p-118 reporter activity was DHT-dependent, and significant responses were identified with 10^{-11} M of DHT with maximal response at 10^{-9} M (Fig. 1C). An anti-androgen, OH-flutamide, antagonized the DHT-induced responses (Fig. 1D).

3.2. Enhancement of DHT responsive transcription in the presence of ERα

The observed increase in mPSP94-p1202 activity treated with DHT at 10^{-9} M was about 2.5 fold of the control, which was lower than that with mPSP94p-118. When an ERα expression vector was co-transfected in CHO cells along with the AR expression vector, the mPSP94p-1202 reporter activity in response to DHT increased significantly, but did not alter PSP94-p118-luc activity. Increased levels of ERα transfection resulted in higher PSP94-1202 activity in response to androgens (Fig. 2A). Transfection of ERβ, on the other hand, did not alter response to androgens. ICI 182780 suppressed the androgen-induced promoter activity of mPSP94 while E_2 administration did not alter activity (Fig. 2B).

3.3. ERE-like motifs in the 5′f region of mPSP94 gene

The enhancing effects of ERα were examined with successive truncated luciferase reporters (Fig. 3A). Significant enhancement was observed with PSP94p-1202 and -450 but not with -200 or -118. Since there are two ERE-like motifs at positions −435 and −216 in the promoter region, it is possible that these sequences may be involved in the ER-dependent enhancement of testosterone responses. When both ERE-like motifs were deleted in the PSP94p-450 reporter, the expected enhancement with ERα was lost, while deletions of only one of the EREs did not affect the enhancing effect (Fig. 3B).

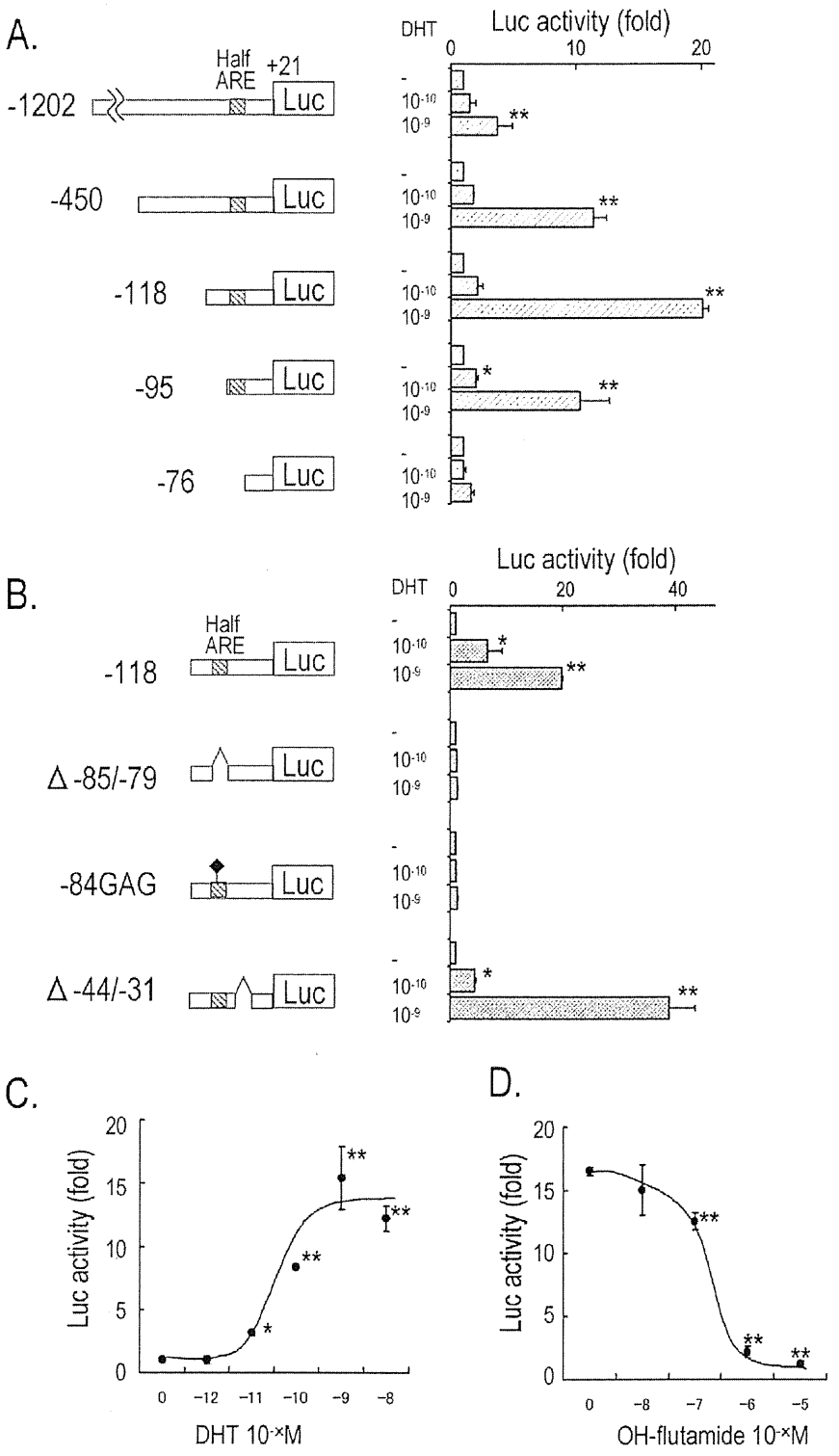

Fig. 1. DHT-dependent promoter activity of the mPSP94 gene in CHO cells. (A) Successive truncated fragments of the 5′f region from mPSP94 were inserted into a luciferase reporter. Position numbers were assigned based on the transcription start site (+1). Reporter plasmids (300 ng) and 30 ng of pSG5-hAR were transfected. DHT was administered at concentrations of 10^{-10} and 10^{-9} M. (B) DHT-induced luciferase activities of deletion and point mutants from the mPSP94p-118 reporter. (C) DHT-dose dependent induction of luciferase activity from the mPSP94p-118 reporter. (D) Dose dependent inhibition by OH-flutamide against DHT (10^{-9} M) induced activity. Bar indicates mean ± SEM, $n = 5$. *$p < 0.05$ and **$p < 0.01$ vs. control.

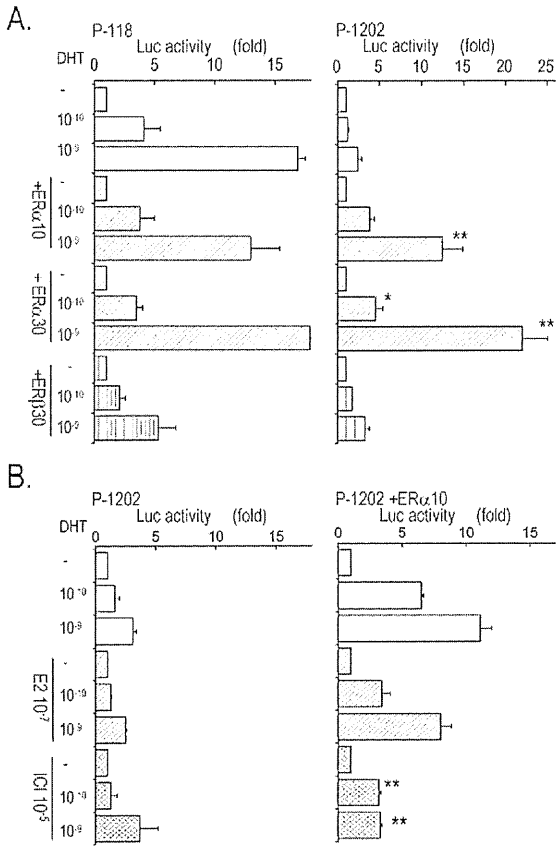

Fig. 2. Effects of ERα transfection upon DHT-dependent promoter activity of the mPSP94 gene in CHO cells. (A) Reporters containing p-118 or p-1202 were transfected along with 30 ng of pSG5-hAR and/or pSG5-hERα (10 or 30 ng) or pSG5-hERβ (30 ng). DHT was administered at concentrations of 10^{-10} or 10^{-9} M. (B) A reporter containing p-1202, pSG5-hAR and/or pSG5-hERα were transfected. DHT was administered at concentrations of 10^{-10} or 10^{-9} M with/without estradiol (E2) at 10^{-7} or ICI182178 at 10^{-5} M. Bar indicates mean ± SEM, $n = 5$. $^{*}p < 0.05$ and $^{**}p < 0.01$ vs. control.

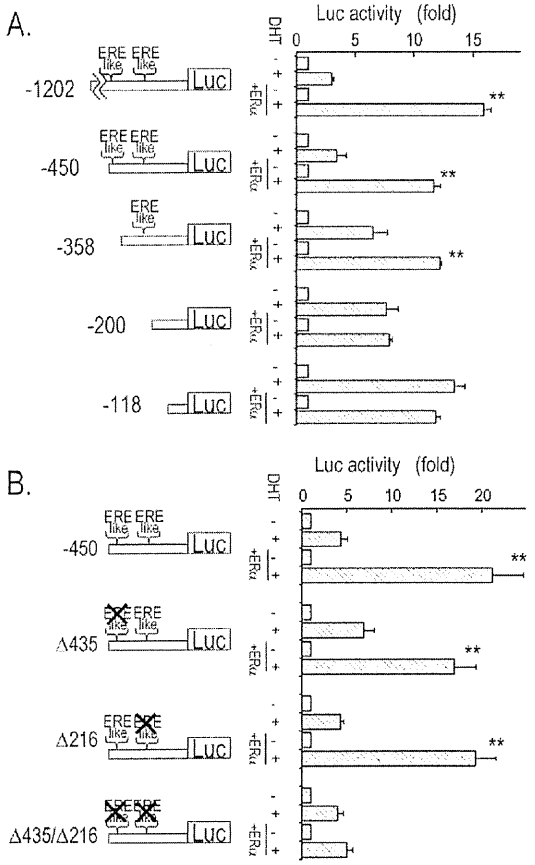

Fig. 3. Requirement of ERE-like motifs for ERα-dependent enhancing effects of androgen responses of the mPSP94 gene in CHO cells. (A) Successive truncated fragments of the mPSP94 promoter were transfected along with pSG5-hAR and pSG5-hERα. DHT was at 10^{-9} M. (B) Deletion mutants of pGL3-mPSP94p-450 were transfected with pSG5-hAR and pSG5-hERα. Bar indicates mean ± SEM, $n = 5$. $^{*}p < 0.05$ and $^{**}p < 0.01$ vs. ER negative control.

3.4. Promoter activity in LNCaP cells

Responses of reporter genes to DHT with successive truncated fragments of the mPSP94 promoter in the LNCaP cell line are summarized in Fig. 4A. Significant inductions were noted in all reporter constructs except mPSP94p-76. We also examined the effect of co-transfection with an ERα expression vector (Fig. 4B). With the mPSPp-118 reporter, ERα did not alter DHT responses, while mPSP94p-450 responses were significantly increased by co-transfection with the ERα expression vector. Co-transfection with the ERα expression vector did not change the response of mPSPp-450(Δ435/Δ216).

4. Discussion

PSP94 is a non-glycosylated and cysteine-rich protein composed of 94 amino acids [3,18,19]. First isolated from human seminal plasma, PSP94 was found to be one of the major prostatic proteins in humans [1]. Although the composition of rodent prostatic proteins is very different from that of humans, PSP94 is commonly expressed in rodents [5,20]. The function of this protein has yet to be fully determined. PSP94 exhibits immunoglobulin-binding capability in order to suppress the activation of B cells [7]. PSP94 may also function as an inhibitor of sperm motility [8].

Prostatic proteins are generally regulated by androgens. When the expression of proteins secreted from the mouse prostate was examined in our previous study, we found that all proteins were indeed significantly reduced just one week following castration of the animal but increased following androgen administration [21]. Some genes may be regulated by the direct interaction of liganded AR and promoter/enhancer regions of the gene, while other changes would be secondary or tertiary events along with involution and regeneration of the prostate tissue. In the case of PSP94, testosterone administration increased mRNA levels in castrated mice by a factor of 38 in just 24 h, suggesting that gene expression was directly controlled by androgens. PSP94 mRNA is expressed in ventral prostate as well as dorso-lateral prostate in the mouse, but is localized specifically in the dorso- and lateral-prostate lobes in the rat. In humans, the expression of PSP94 was not restricted to the prostate but was additionally detected in secretions from the respiratory tract, gastric fluid and other secretory tissues [18]. Since expression was very specific to the prostate in rodents, the promoter/enhancer structure of mPSP94 gene has drawn significant interest as potential gene targeting tools. It has been demonstrated that a 3.8 kb of the 5′f region was capable of directing gene expression in a prostate tissue specific mode, that was additionally ventral- and dorso-lateral lobe specific, in a transgenic mouse model [16].

Androgens regulate their responsive genes via intracellular ARs. Upon ligand binding, ARs interact with specific DNA sequences,

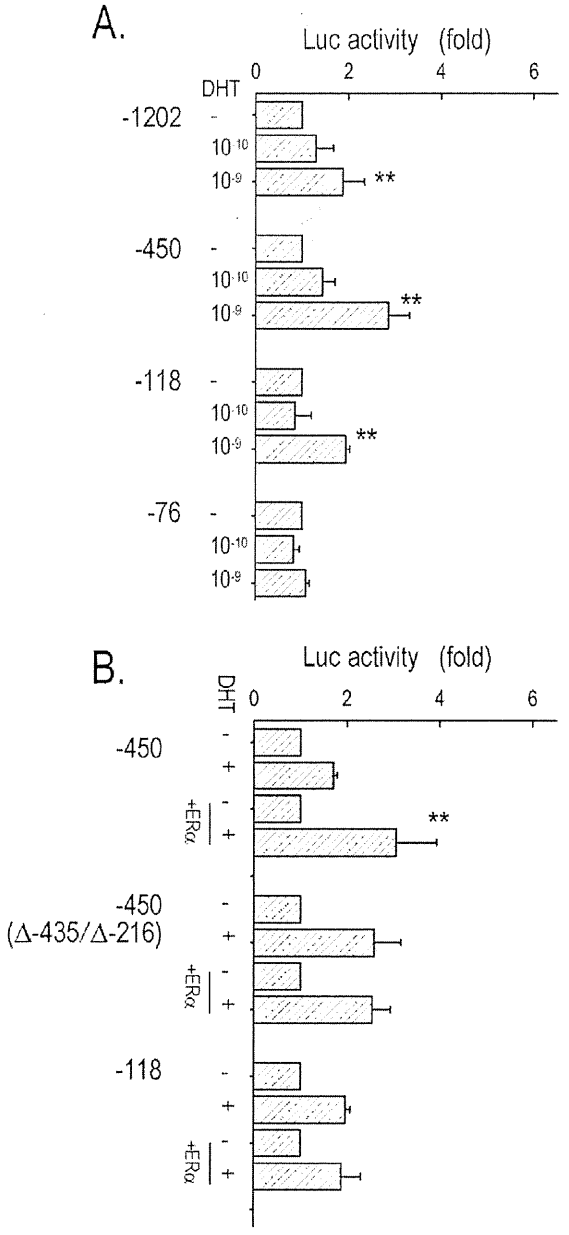

Fig. 4. DHT-dependent promoter activity of the mPSP94 gene in LNCaP cells. (A) Luciferase reporter constructs containing truncated fragments of the mPSP94 promoter were transfected and DHT was administered at concentrations of 10^{-10} and 10^{-9} M. (B) Reporter constructs containing p-450, ERE deleted p-450(Δ435/Δ 216) and p-118 were transfected with pSG5-hERα. DHT was at 10^{-9} M. Bar indicates mean ± SEM, $n = 5$. $^{**}p < 0.01$ vs. DHT negative control (A) and vs. ERα negative control (B).

known as AREs, and thus regulate the transcriptional activity of genes [22,23]. Steroid hormone receptors generally bind to DNA elements consisting of inverted repeats of six base pairs by three nucleotide spacers. The consensus hexametric sequence for AR is TGTTCT, which is identical to the glucocorticoid and progesterone responsive element. Previous investigations have revealed that AREs are divided into two categories; one interacts with glucocorticoids, mineralocorticoids and progesterone receptors, in addition to ARs, while the other is specific to ARs [24,25]. Previously described sequence data suggested that AR specific AREs tend to be organized as partial direct repeats rather than inverted repeats of the consensus hexametric repeat [22]. In mPSP94, we found an ARE candidate, TACCTAnnnTGTTCT that contains a half consensus ARE at position −93. Since androgen-dependent luciferase reporter activity was completely lost when this element was deleted or mutated, this motif between positions −93 and −79 appears to represent the functional ARE, although further studies are needed to determine if there are any direct interactions between this ARE-like sequence and AR. In the present study we primarily utilized CHO cells for the promoter assay since it is easy to perform transient transfection experiments in high efficiencies with this mammalian cell line. In addition, we used LNCaP, a human prostate adenocarcinoma cell line, to confirm the biological relevance of the promoter activity. LNCaP is an AR positive cell line that grows responding to testosterone and has been frequently used to study the androgen responsive gene regulation [26].

It has been demonstrated that combined administration of androgen and estrogen synergistically enhanced the development of prostatic hyperplasia and cancer in Noble rats as well as in chemical carcinogen-treated F344 rats [27,28]. In the previous study, we examined the expression of prostatic protein genes such as probasin and kallikrein S3 to understand the molecular mechanism underling the androgen plus estrogen effect [29]. We found that estradiol enhanced the androgen dependent expression of prostatic genes along with increase in ERα expression, which suggested that the elevated prostatic ERα may contribute to the enhancing effects. In the present study, we tested this hypothesis with PSP94 promoter and found that the androgen-dependent induction was enhanced by the presence of ERα while administration of estradiol did not change the transcription levels. In the PSP94 promoter, there are two ERE-like motifs that potentially interact with ERs at positions −435 and −216, ctannAnnnTGACCT and gGGnncnnnTGACCa, where the consensus ERE is ARGnnAnnnTGACCY. Results arising from deletion mutants indicated that at least one ERE similar motif is enough for the enhancement of androgen responses. These enhanced responses, however, did not exceed the degree of responses with the mPSP94p-118 reporter. Since reporters containing longer 5′f region displayed lower responses, it appears that the distal region of the promoter has suppressive function on the transcription and the presence of ERα may release the suppression. In normal adult prostate tissue, ERα expression is localized to stromal cells and ERβ is in epithelia [30]. In PC, however, epithelial expression of ERα increases while ERβ expression is reduced or lost [31–33]. During the development of PC, increasing ERα expression might enhance some critical androgen responsive genes related to prostatic carcinogenesis by the similar mechanisms found in the present study.

References

[1] P.A. Abrahamsson, H. Lilja, Three predominant prostatic proteins, Andrologia 22 (Suppl. 1) (1990) 122–131.
[2] J. Tremblay, G. Frenette, R.R. Tremblay, A. Dupont, M. Thabet, J.Y. Dube, Excretion of three major prostatic secretory proteins in the urine of normal men and patients with benign prostatic hypertrophy or prostate cancer, Prostate 10 (1987) 235–243.
[3] S. Garde, J.E. Fraser, N. Nematpoor, R. Pollex, C. Morin, A. Forte, S. Rabbani, C. Panchal, M.B. Gupta, Cloning expression, purification and functional characterization of recombinant human PSP94, Protein Expr. Purif. 54 (2007) 193–203.
[4] Y. Imasato, T. Onita, M. Moussa, H. Sakai, F.L. Chan, J. Koropatnick, J.L. Chin, J.W. Xuan, Rodent PSP94 gene expression is more specific to the dorsolateral prostate and less sensitive to androgen ablation than probasin, Endocrinology 142 (2001) 2138–2146.
[5] A. Thota, M. Karajgikar, W. Duan, M.Y. Gabril, F.L. Chan, Y.C. Wong, H. Sakai, J.L. Chin, M. Moussa, J.W. Xuan, Mouse PSP94 expression is prostate tissue-specific as demonstrated by a comparison of multiple antibodies against recombinant proteins, J. Cell Biochem. 88 (2003) 999–1011.
[6] M. Kamada, H. Mori, N. Maeda, S. Yamamoto, K. Kunimi, M. Takikawa, M. Maegawa, T. Aono, S. Futaki, S.S. Koide, beta-Microseminoprotein/prostatic secretory protein is a member of immunoglobulin binding factor family, Biochim. Biophys. Acta 1388 (1998) 101–110.

[7] A. Kumar, D.D. Jagtap, S.D. Mahale, M. Kumar, Crystal structure of prostate secretory protein PSP94 shows an edge-to-edge association of two monomers to form a homodimer, J. Mol. Biol. 397 (2010) 947–956.
[8] N. Aoki, A. Sakiyama, M. Deshimaru, S. Terada, Identification of novel serum proteins in a Japanese viper: homologs of mammalian PSP94, Biochem. Biophys. Res. Commun. 359 (2007) 330–334.
[9] R.J. Matusik, C. Kreis, P. McNicol, R. Sweetland, C. Mullin, W.H. Fleming, J.G. Dodd, Regulation of prostatic genes: role of androgens and zinc in gene expression, Biochem. Cell Biol. 64 (1986) 601–607.
[10] K.B. Cleutjens, C.C. van Eekelen, H.A. van der Korput, A.O. Brinkmann, J. Trapman, Two androgen response regions cooperate in steroid hormone regulated activity of the prostate-specific antigen promoter, J. Biol. Chem. 271 (1996) 6379–6388.
[11] Z. Wang, R. Tufts, R. Haleem, X. Cai, Genes regulated by androgen in the rat ventral prostate, Proc. Natl. Acad. Sci. U.S.A. 94 (1997) 12999–13004.
[12] P.H. Riegman, R.J. Vlietstra, J.A. van der Korput, A.O. Brinkmann, J. Trapman, The promoter of the prostate-specific antigen gene contains a functional androgen responsive element, Mol. Endocrinol. 5 (1991) 1921–1930.
[13] S. Zhang, P.E. Murtha, C.Y. Young, Defining a functional androgen responsive element in the 5′ far upstream flanking region of the prostate-specific antigen gene, Biochem. Biophys. Res. Commun. 231 (1997) 784–788.
[14] S. Kasper, P.S. Rennie, N. Bruchovsky, L. Lin, H. Cheng, R. Snoek, K. Dahlman-Wright, J.A. Gustafsson, R.P. Shiu, P.C. Sheppard, R.J. Matusik, Selective activation of the probasin androgen-responsive region by steroid hormones, J. Mol. Endocrinol. 22 (1999) 313–325.
[15] P.S. Rennie, N. Bruchovsky, K.J. Leco, P.C. Sheppard, S.A. McQueen, H. Cheng, R. Snoek, A. Hamel, M.E. Bock, B.S. MacDonald, Characterization of two cis-acting DNA elements involved in the androgen regulation of the probasin gene, Mol. Endocrinol. 7 (1993) 23–36.
[16] M.Y. Gabril, T. Onita, P.G. Ji, H. Sakai, F.L. Chan, J. Koropatnick, J.L. Chin, M. Moussa, J.W. Xuan, Prostate targeting: PSP94 gene promoter/enhancer region directed prostate tissue-specific expression in a transgenic mouse prostate cancer model, Gene Ther. 9 (2002) 1589–1599.
[17] S. Kitamura, T. Suzuki, S. Ohta, N. Fujimoto, Antiandrogenic activity and metabolism of the organophosphorus pesticide fenthion and related compounds, Environ. Health Perspect. 111 (2003) 503–508.
[18] J.W. Xuan, D. Wu, Y. Guo, S. Garde, D.T. Shum, M. Mbikay, R. Zhong, J.L. Chin, Molecular cloning and gene expression analysis of PSP94 (prostate secretory protein of 94 amino acids) in primates, DNA Cell Biol. 16 (1997) 627–638.
[19] J.W. Xuan, J. Kwong, F.L. Chan, M. Ricci, Y. Imasato, H. Sakai, G.H. Fong, C. Panchal, J.L Chin, cDNA, genomic cloning, and gene expression analysis of mouse PSP94 (prostate secretory protein of 94 amino acids), DNA Cell Biol. 18 (1999) 11–26.
[20] J. Kwong, J.W. Xuan, H.L. Choi, P.S. Chan, F.L. Chan, PSP94 (or beta-microseminoprotein) is a secretory protein specifically expressed and synthesized in the lateral lobe of the rat prostate, Prostate 42 (2000) 219–229.
[21] N. Fujimoto, Y. Akimoto, T. Suzuki, S. Kitamura, S. Ohta, Identification of prostatic-secreted proteins in mice by mass spectrometric analysis and evaluation of lobe-specific and androgen-dependent mRNA expression, J. Endocrinol. 190 (2006) 793–803.
[22] F. Claessens, S. Denayer, N. Van Tilborgh, S. Kerkhofs, C. Helsen, A. Haelens, Diverse roles of androgen receptor (AR) domains in AR-mediated signaling, Nucl. Recept. Signal. 6 (2008) e008.
[23] E.C. Bolton, A.Y. So, C. Chaivorapol, C.M. Haqq, H. Li, K.R. Yamamoto, Cell- and gene-specific regulation of primary target genes by the androgen receptor, Genes Dev. 21 (2007) 2005–2017.
[24] P.S. Nelson, N. Clegg, H. Arnold, C. Ferguson, M. Bonham, J. White, L. Hood, B. Lin, The program of androgen-responsive genes in neoplastic prostate epithelium, Proc. Natl. Acad. Sci. U.S.A. 99 (2002) 11890–11895.
[25] F. Claessens, G. Verrijdt, E. Schoenmakers, A. Haelens, B. Peeters, G. Verhoeven, W. Rombauts, Selective DNA binding by the androgen receptor as a mechanism for hormone-specific gene regulation, J. Steroid Biochem. Mol. Biol. 76 (2001) 23–30.
[26] J. Veldscholte, C.A. Berrevoets, E. Mulder, Studies on the human prostatic cancer cell line LNCaP, J. Steroid Biochem. Mol. Biol. 49 (1994) 341–346.
[27] R.L. Noble, The development of prostatic adenocarcinoma in Nb rats following prolonged sex hormone administration, Cancer Res. 37 (1977) 1929–1933.
[28] K. Suzuki, Y. Takezawa, T. Suzuki, S. Honma, H. Yamanaka, Synergistic effects of estrogen with androgen on the prostate—effects of estrogen on the prostate of androgen-administered rats and 5-alpha-reductase activity, Prostate 25 (1994) 169–176.
[29] N. Fujimoto, H. Honda, T. Suzuki, S. Kitamura, Estrogen enhancement of androgen-responsive gene expression in hormone-induced hyperplasia in the ventral prostate of F344 rats, Cancer Sci. 95 (2004) 711–715.
[30] T. Tsurusaki, D. Aoki, H. Kanetake, S. Inoue, M. Muramatsu, Y. Hishikawa, T. Koji, Zone-dependent expression of estrogen receptors alpha and beta in human benign prostatic hyperplasia, J. Clin. Endocrinol. Metab. 88 (2003) 1333–1340.
[31] G.S. Yang, Y. Wang, P. Wang, Z.D. Chen, Expression of oestrogen receptor-alpha and oestrogen receptor-beta in prostate cancer, Chin. Med. J. (Engl.) 120 (2007) 1611–1615.
[32] M. Royuela, M.P. de Miguel, F.R. Bethencourt, M. Sanchez-Chapado, B. Fraile, M.I. Arenas, R. Paniagua, Estrogen receptors alpha and beta in the normal, hyperplastic and carcinomatous human prostate, J. Endocrinol. 168 (2001) 447–454.
[33] L.G. Horvath, S.M. Henshall, C.S. Lee, D.R. Head, D.I. Quinn, S. Makela, W. Delprado, D. Golovsky, P.C. Brenner, G. O'Neill, R. Kooner, P.D. Stricker, J.J. Grygiel, J.A. Gustafsson, R.L. Sutherland, Frequent loss of estrogen receptor-beta expression in prostate cancer, Cancer Res. 61 (2001) 5331–5335.

Biochemical and Biophysical Research Communications 412 (2011) 366–372

Contents lists available at ScienceDirect

Biochemical and Biophysical Research Communications

journal homepage: www.elsevier.com/locate/ybbrc

Genistein promotes DNA demethylation of the steroidogenic factor 1 (SF-1) promoter in endometrial stromal cells

Hiroshi Matsukura [a], Ken-ichi Aisaki [b], Katsuhide Igarashi [b], Yuko Matsushima [b], Jun Kanno [b], Masaaki Muramatsu [a], Katsuko Sudo [a,c], Noriko Sato [a,*]

[a] Department of Molecular Epidemiology, Medical Research Institute, Tokyo Medical and Dental University, 2-3-10 Kanda-surugadai, Chiyoda-ku, Tokyo 101-0062, Japan
[b] Division of Cellular and Molecular Toxicology, National Institute of Health Sciences, 1-18-1 Kamiyoga, Setagaya-ku, Tokyo 158-8501, Japan
[c] Animal Research Center, Tokyo Medical University, 6-1-1 Shinjuku, Shinjuku-ku, Tokyo 160-8402, Japan

ARTICLE INFO

Article history:
Received 21 July 2011
Available online 29 July 2011

Keywords:
Genistein
DNA methylation
Ovariectomized mice
Primary culture
Steroidogenic factor 1
High-resolution melting analysis

ABSTRACT

It has recently been demonstrated that genistein (GEN), a phytoestrogen in soy products, is an epigenetic modulator in various types of cells; but its effect on endometrium has not yet been determined. We investigated the effects of GEN on mouse uterine cells, *in vivo* and *in vitro*. Oral administration of GEN for 1 week induced mild proliferation of the endometrium in ovariectomized (OVX) mice, which was accompanied by the induction of steroidogenic factor 1 (SF-1) gene expression. GEN administration induced demethylation of multiple CpG sites in the SF-1 promoter; these sites are extensively methylated and thus silenced in normal endometrium. The GEN-mediated promoter demethylation occurred predominantly on the luminal side, as opposed to myometrium side, indicating that the epigenetic change was mainly shown in regenerated cells. Primary cultures of endometrial stromal cell colonies were screened for GEN-mediated alterations of DNA methylation by a high-resolution melting (HRM) method. One out of 20 colony-forming cell clones showed GEN-induced demethylation of SF-1. This clone exhibited a high proliferation capacity with continuous colony formation activity through multiple serial clonings. We propose that only a portion of endometrial cells are capable of receiving epigenetic modulation by GEN.

1. Introduction

Genistein (GEN), a major phytoestrogen in dietary soy, is a substantial component of the typical Asian and Western vegetarian diets, as well as recently developed infant soy milk formulas. There are several well known potential health benefits of GEN intake [1,2], one of which is an apparent decreased risk of breast and prostate cancers, based on human observational studies [1,3]. But GEN also paradoxically stimulates growth of breast cancer cells in culture [2] and uterine enlargement in rodents [4]. These effects may be mediated through estrogen receptor interactions and/or modulation of endogenous estrogen metabolism [5,6]. Since GEN can bind to estrogen receptors (ERs) α and β, with a stronger affinity to ERβ [5], it is categorized as a phyto-selective estrogen receptor modulator (SERM) [6,7]. The variations in GEN's agonistic or antagonistic effects may be affected by variations in endogenous estrogen levels. Previous studies have not determined whether the pleiotropic effects of GEN involve distinct epigenetic alteration. Recently, GEN was shown to alter DNA methylation in various types of cells, including ES cells [8], but most studies have been performed using cancer cell lines [9–11]. There have been few reports of the effects of GEN on DNA methylation in intact cells or *in vivo* [12]. In the present study, we utilized a uterotropic assay in ovariectomized (OVX) mice, as a model system to analyze epigenetic regulation by GEN.

In a previous study, high-dose GEN administration to OVX rats resulted in increased uterine weight and changed endometrial cell gene expression [6]. However, no epigenetic alterations were demonstrated under this condition. We selected the steroidogenic factor 1 (SF-1; official symbol: Nr5a1) gene as a target for the methylation analysis. SF-1 is an orphan nuclear receptor and transcription factor for key enzymes involved in steroidogenesis, such as StAR, Cyp11a1 (p450scc), Cyp17a1 (p450c17), and Cyp19a1 (aromatase) [13]. The SF-1 gene is not expressed in normal endometrium; however, SF-1 expression is reactivated in the disease state of human ectopic endometriosis, in which the SF-1 promoter is abnormally demethylated by an unknown mechanism [14]. The subsequent enhancement of steroidogenic genes and resultant local steroidogenesis are proposed to be important etiologies [15]. Therefore, we hypothesized that in mouse endometrial cells,

* Corresponding author. Fax: +81 3 5280 8058.
E-mail addresses: hmatsukura.epi@mri.tmd.ac.jp (Hiroshi Matsukura), nsato.epi@tmd.ac.jp (N. Sato).

0006-291X/$ - see front matter © 2011 Elsevier Inc. All rights reserved.
doi:10.1016/j.bbrc.2011.07.104

SF-1 might be subjected to epigenetic modulation by some external stimuli. Here we show that the SF-1 promoter was demethylated *in vivo* and *in vitro* by GEN treatment. This is the first demonstration of a phytoestrogen altering the epigenetic state of adult endometrium.

2. Materials and methods

2.1. Ethics statement

All procedures described here were performed according to protocols approved by the Animal Care Committee of the National Institute of Health Sciences, and Tokyo Medical and Dental University (No. 0110306A).

2.2. Oral administration of genistein to ovariectomized mice

C57BL/6JJmsSlc female mice (SLC) were used in this study. All mice were fed a phytoestrogen-free diet (Oriental Yeast) and were ovariectomized (OVX) 2 weeks prior to the genistein (GEN) treatment. OVX mice were divided into three different treatment groups, each consisting of 3–5 independent replicates, which orally received low-dose GEN (60 mg/kg/day), high-dose GEN (200 mg/kg/day), or vehicle (0.5% CMC-Na (Maruishi Pharmaceutical); 5 ml/kg/day) for 1 week. At the end of treatment (9 weeks of age), all mice were euthanized by exsanguination under ether anesthesia.

2.3. Uterotrophic assay and gene expression study after oral administration of genistein

Whole uteri were harvested, blotted, and weighted. Each uterus was divided into two horns, immediately placed into 2 ml plastic tubes of RNAlater solution (Ambion), and stored at 4 °C. From each sample, one horn was processed for mRNA expression analyses; RNAlater was replaced with 1.0 ml of RLT buffer (Qiagen), and the horn was homogenized by addition of a 5 mm diameter Zirconium bead (Funakoshi) and shaking with a MixerMill 300 (Qiagen) at 20 Hz for 5 min (only the outermost row of the shaker box was used). Further sample preparation and analysis were performed as previously described [16]. mRNA expressions were analyzed using Affymetrix Murine Genome 430 2.0 GeneChips, and calculated as copy number per cell by the Percellome method [16]. The second uterine horn of each sample was subjected to genomic DNA isolation.

2.4. Isolation of colony-forming cells derived from intact uteri

Five 8- to 9-week-old C57BL/6JJmsSlc female mice (SLC) were euthanized by cervical dislocation and whole uteri were harvested. Uterine horns were collected in Dulbecco's modified Eagle's medium/Hams F-12 (DMEM/F-12; Nacalai Tesque) containing 0.05 mg/ml gentamicin (Sigma–Aldrich). Each horn was dissected longitudinally and the endometrial tissue was divided into two portions: the luminal side and the myometrium side. A single cell suspension of endometrial cells was obtained using enzymatic digestion and mechanical means adapted from Chan et al. [17]. The tissue samples were minced and dissociated in 500 μl DMEM/F-12 containing 0.12 mg/ml (0.56 Wünsch U/ml) Blendzyme 2 and 40 μg/ml deoxyribonuclease type I (both from Roche Applied Science) in a shaking incubator (~90 rpm) at 37 °C. At 15 min intervals, the digests were pipetted to promote separation and cell dissociation was monitored microscopically. After 45 min, debris was filtered out using a 40-μm sieve (BD Biosciences). The single-cell suspensions were collected in DMEM/F-12 containing 10% FBS, 0.05 mg/ml gentamicin and stored on ice. Then the sieves were backwashed, and myometrial and glandular debris were further digested to single cells for 45 min as described above. All cell suspensions were filtered as described above, and combined. To remove erythrocytes, the cells were resuspended in 500 μl of HLB solution (Immuno Biological Laboratories) and incubated for 3 min. After washing twice with PBS, viable cell numbers were counted with trypan blue (Sigma–Aldrich). Cells were seeded on gelatin (0.1%, Sigma–Aldrich)-coated dishes at various densities of $0.1–3 \times 10^5$ cell/60-mm dish. After 14 days, non-overlapping clones were distinguished. Primary cell clones were expanded in DMEM/F-12 containing 5% FBS (SAFC Biosciences) and 0.05–0.1 mg/ml gentamicin, on gelatin-coated dishes.

2.5. Serial cloning of colony-forming cell clones

Self renewal was assessed by serial cloning of individual clones as described by Gargett et al. [18]. Cells were seeded on gelatin-coated 100-mm dishes at 10 cells/cm^2 (600 cells/100-mm dish). Culture medium was changed every 4 days and secondary clones formed distinct colonies by 14 days after plating. Secondary clones were similarly recloned to generate tertiary clones, and were also expanded in the same manner as the primary culture.

2.6. In vitro genistein exposure to colony-forming cells

From 70 isolated cell clones, we selected 20 clones from colonies that were composed of fibroblastic-shaped, homogenous cells with an average doubling time of less than 100 h. The selected clonal cells, whose passage number was less than 10, were subjected to *in vitro* GEN exposure. Cells were seeded on gelatin-coated 60-mm dishes, treated with or without 10 μM of GEN (dissolved in dimethylsulfoxide (DMSO)) in DMEM/F-12 containing 5% FBS and 0.05 mg/ml gentamicin for 7 days. The final DMSO concentration was 0.02%. The culture medium was changed every 2 days.

2.7. Genomic DNA preparation and bisulfite sequencing

Genomic DNA was isolated using a QIAamp DNA Mini Kit (QIAGEN) and 180 ng–1 μg was subjected to sodium bisulfite modification with a EpiTect Bisulfite Kit (QIAGEN) according to manufacturer's protocols. Bisulfite sequencing primers are shown in **Supplementary Table 1**. PCR products were cloned into the pT7 blue T vector (Novagen) and transformed into *Escherichia coli*. Plasmid DNA from positive colonies was purified and sequenced at the Tokyo Medical and Dental University Genome Laboratory (Tokyo, Japan). Sequence and statistical analyses were performed with the QUantification tool for Methylation Analysis; http://quma.cdb.riken.jp/top/quma_main_j.html [19]. The statistical significance of the difference between two bisulfite sequence groups at each CpG site was evaluated with Fisher's exact test.

2.8. Screening of DNA methylation status by high-resolution melting assay

All assays were performed on the LightCycler 480 using the LightCycler 480 High Resolution Melting Master kit, according to the manufacturer's instructions. Primers, designed using LightCycler Probe Design Software 2.0 (All, Roche Applied Science) are shown in **Supplementary Table 1**. All data were analyzed using LightCycler Gene Scanning Software.

2.9. Statistical analysis

Data are shown as means ± SD. Unpaired *t*-tests were used to compare the significance between two groups. Statistical analysis

was performed using Dr. SPSS 2 for Windows. Results were considered statistically significant at a P value of <0.05.

3. Results

3.1. Effects of genistein in uteri of ovariectomized (OVX) mice

OVX mice were fed with either vehicle (control) or low (60 mg/kg) or high (200 mg/kg) doses of GEN for 7 days and blotted uterus weights were determined (Fig. 1A). Compared to the control, low-dose GEN treatment did not significantly increase the uterus weight; high-dose treatment induced a slight but significant uterus enlargement (1.4-fold of control; $P < 0.005$). We then determined the mRNA expression levels of SF-1 (Fig. 1B) and steroidogenic genes (Fig. 1C–F) by the Percellome method. The mRNA levels of these genes were very low in the endometria from control and low-dose GEN-treatment groups, but were significantly increased (still less than one copy per cell on average) in the high-dose treatment group ($P < 0.05$), indicating that high-doses of GEN induced expression of these genes. Next, we determined the methylation status of SF-1 in

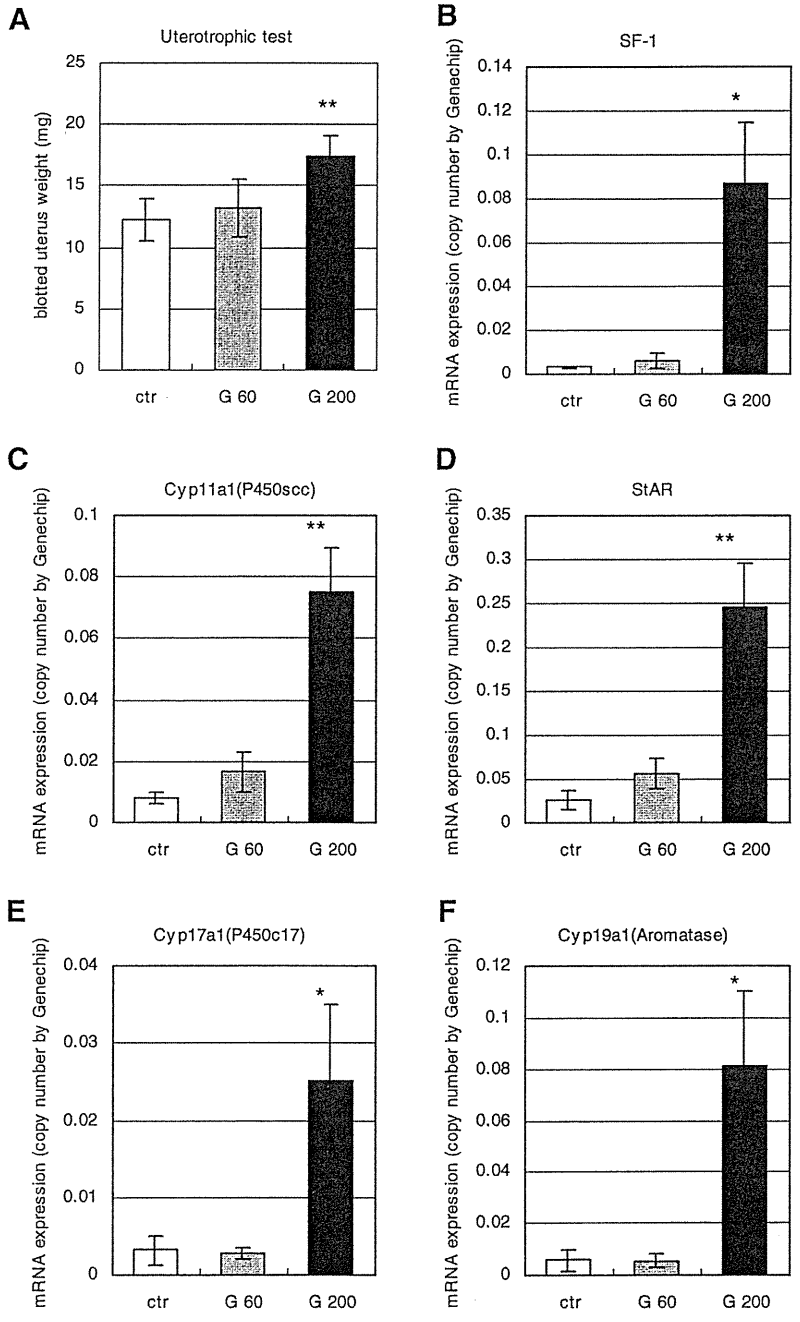

Fig. 1. Genistein induced endometrial regeneration and SF-1 mRNA expression in uterine tissue of OVX mice. (A) Blotted uterine weights were recorded. Control and GEN-treated groups comprised five and four mice, respectively. ctr; control, G 60; GEN 60 mg/kg/d, G200; GEN 200 mg/kg/d. (B–F) mRNA expressions of steroidogenic genes were determined using GeneChip analysis and were calculated by the Percellome method. Y axis indicates mRNA expression as copy number per cell. (B) SF-1 was determined by 1418315_at, (C) Cyp11a1 by 1439947_at, (D) StAR by 1418729_at, (E) Cyp17a1 by 1417017_at, and (F) Cyp19a1 by 1449920_at. *Statistically significant at $P < 0.05$. **Statistically significant at $P < 0.005$.

the total uterus tissues of the three groups of mice by bisulfite sequencing (Fig. 2A–C). There were 15 CpG sites spanning −272 to +199 of the promoter and the 5′-UTR (exon 1) region of SF-1. The percentages of total methylated CpG sites in this region, in control, and low and high-dose GEN, were 78.3%, 73.9%, and 54.4%, respectively, indicating that GEN dose-dependently induced demethylation in this region. Most CpG sites in the 5′-UTR (exon1) were demethylated by high-dose GEN. In particular, the methylation levels of 5 CpG sites between +45 and +89 were significantly lower in high-dose GEN than in control (Fisher's exact test, $P < 0.01$). We further split the endometrium to separate the luminal side (LU) from the basilar myometrial side (MY), and both specimens were separately subjected to bisulfite sequencing. This procedure was applied to the samples from the GEN-treated groups but not to control samples due to uterus atrophy. In low-dose GEN treated mice, the mean methylation levels of LU and MY were 84.8% and 65.0%, respectively (not shown). In high-dose GEN treated mice, the mean methylation levels of LU and MY were 42.1% and 66.7%, respectively (Fig. 2D). Thus, the demethylation induced by high-dose GEN occurred predominantly in the LU, rather than in the MY.

3.2. Effect of genistein on primary endometrial cell culture

In order to study the SF-1 promoter methylation at the cellular level, we employed an endometrial cell primary culture. Intact murine endometrium were divided into LU and MY portions, and cells were separately isolated. Primary cell clones were established by colony-formation, following the plating of a serially-titrated cell suspension (see Section 2). Efficient isolated colony formation was achieved with cells seeded at a density of 4,500–15,300 cells/cm^2. For LU and MY, the average frequencies of colony appearance were 7.5 per 10^5 cells and 15 per 10^5 cells, respectively. The growth curves of representative clones derived from LU and MY are shown in Fig. 3. Cell clones with highest and lowest proliferative activities were obtained from LU and MY, separately. More highly proliferative cells were obtained from MY than from LU (Fig. 3A and C). We selected 20 highly proliferative clones for further study (see Section 2). Two rapid growing clones obtained from MY showed self-renewal activity when secondarily seeded at a very low cell density (10 cells/cm^2) (not shown). To screen for primary cultured cells that responded to GEN, we set up a high-resolution melting (HRM) assay that identified region-specific methylation levels. The region analyzed by HRM assay exclusively contained the 7 CpG sites between +19 and +89 bp that were most differentially demethylated following oral administration of GEN (Fig. 2). Each clone was treated with or without GEN for 1 week; cells treated with a similar concentration of DMSO served as control. Among the 20 clones that we screened, only one GEN-treated clone (No. 16) exhibited a significant shift in the melting curve compared to control cells (Fig. 4A). This clone had the highest proliferation

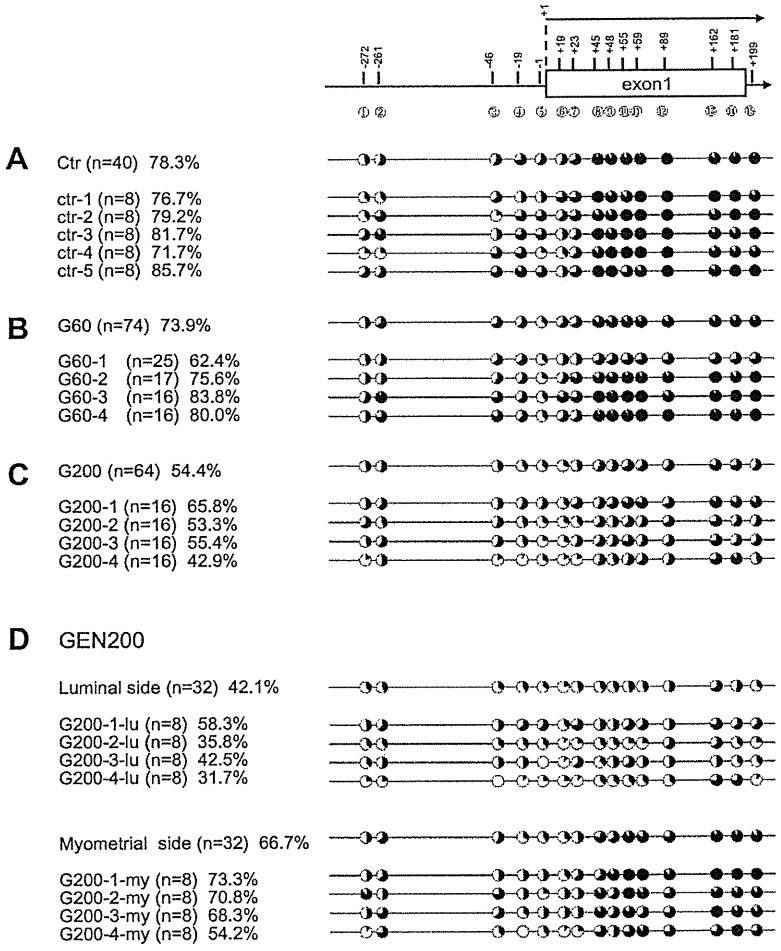

Fig. 2. Genistein induced demethylation of the SF-1 gene promoter in endometrial tissues of OVX mice. The schematic diagram indicates CpG locations on the SF-1 promoter region, spanning 5′-flanking to exon 1. The CpG position relative to the first base of exon 1 (+1) is shown. The bisulfite sequencing fragment contains 15 CpG sites. The black inlay represents the mean methylation levels of each CpG, and the left panel contains the number of sequenced clones and the mean methylation level of all CpGs. Summarized methylation results are shown at the top. (A–C) Difference in methylation levels between (A) vehicle (control), (B) low-dose GEN (60 mg/kg/d), and (C) high-dose GEN (200 mg/kg/d) exposed uteri. (D) Difference in methylation levels between luminal and myometrial sides of a uterus exposed to high-dose GEN.

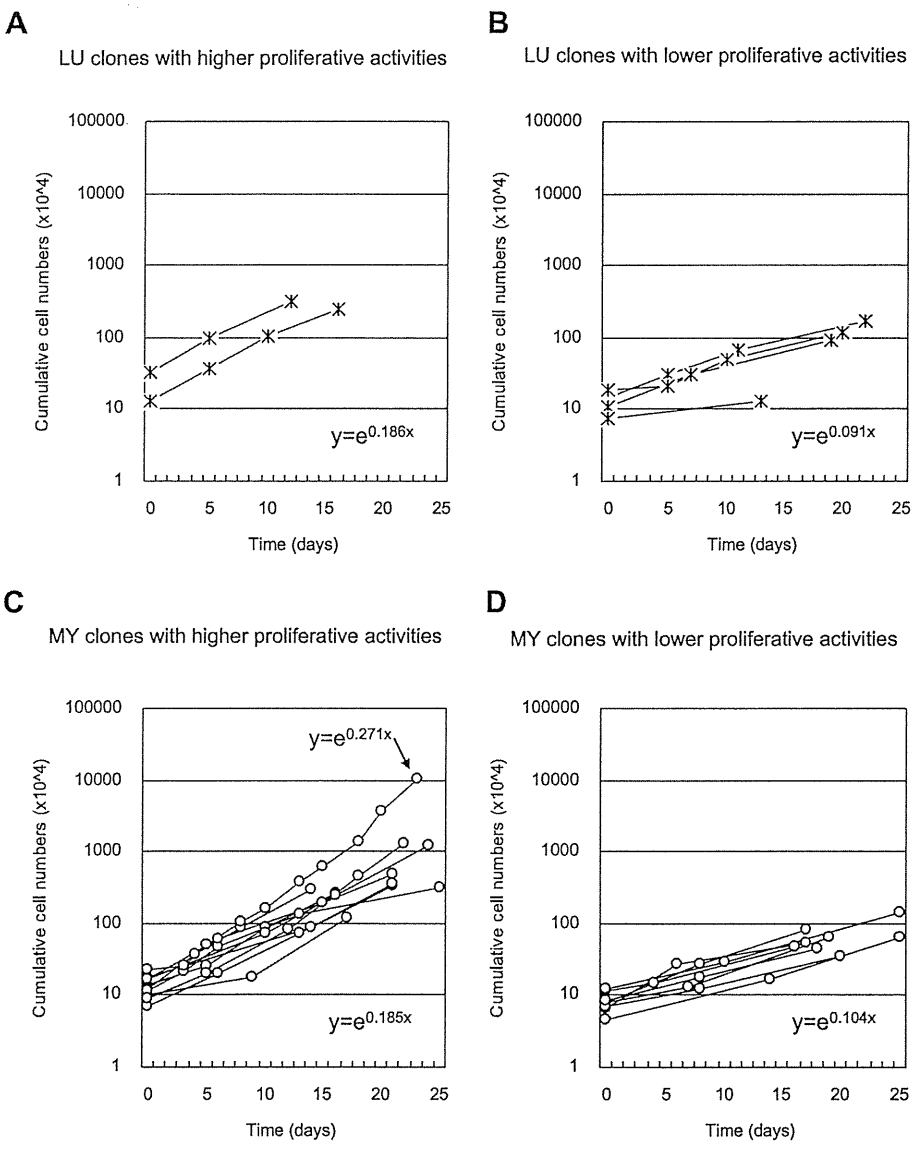

Fig. 3. Proliferation properties of isolated clones: one clone showed highly proliferative activity. Representative growth curves of clones harvested from intact murine endometrium are shown. Formula indicates the slope of fitted growth curves. Clones were divided into two groups: high and low proliferative (see Section 2). A total of 20 highly proliferative clones were analyzed by HRM after *in vitro* GEN treatment. (A, B) Asterisks indicate representative growth curves of cell clones isolated from luminal side. (A) Clones with higher proliferative activities, derived from luminal side. Six highly proliferative clones were obtained in total; 2 representatives are shown. (B) Clones with lower proliferative activities, derived from luminal side. (C, D) Each circle indicates representative growth curves of cell clones isolated from myometrial side. (C) Clones with higher proliferative activities, derived from the myometrial side. In total, 14 highly proliferative clones were obtained; 10 representatives are shown. The arrow indicates the clone with the most rapid growth. (D) Clones with lower proliferative activities, derived from myometrial side.

activity (Fig. 3C, arrow). GEN treatment of the other clones did not result in significant changes to the melting curve patterns (not shown). We further confirmed the methylation status of clone No. 16 by bisulfite sequencing. The percentages of CpG methylation in the SF-1-272 to +199 promoter regions for untreated and GEN-treated cells were 85.0% and 65.8%, respectively (Fig. 4B).

4. Discussion

Growing evidence suggests that the manner in which nutrients can either help maintain health, or conversely, promote disease development may be mediated by epigenetic regulation [12,20]. However, relatively little is known about tissue-specific sensitivity or how much plasticity exists in regards to the effect that a given environmental factor can exert on a certain epigenetic target [20,21]. GEN, a non-nutrient dietary component of soy products, exhibits mixed estrogen agonist and antagonist properties, and multiple functions both *in vivo* and *in vitro* [7,22]. Several animal studies have demonstrated that GEN acts as an epigenetic modulator [20]. We focused on the effects of GEN on endometrium, because endometrium is not only hormone responsive, but also a highly proliferative organ. Epigenetic alterations of proliferative tissue or cells may then be expanded through tissue proliferation. We used OVX rodents, which are a widely used model for studying estrogen withdrawal and replacement [23], as well as for the assessment of endocrine-disrupting chemicals in the environment [4]. In our experiment, GEN induced proliferation of the endometrium and increased uterine weight (Fig. 1A) to extents similar to those previously reported in OVX rats [4]. Our findings also suggested that GEN treatment induced marked demethylation of

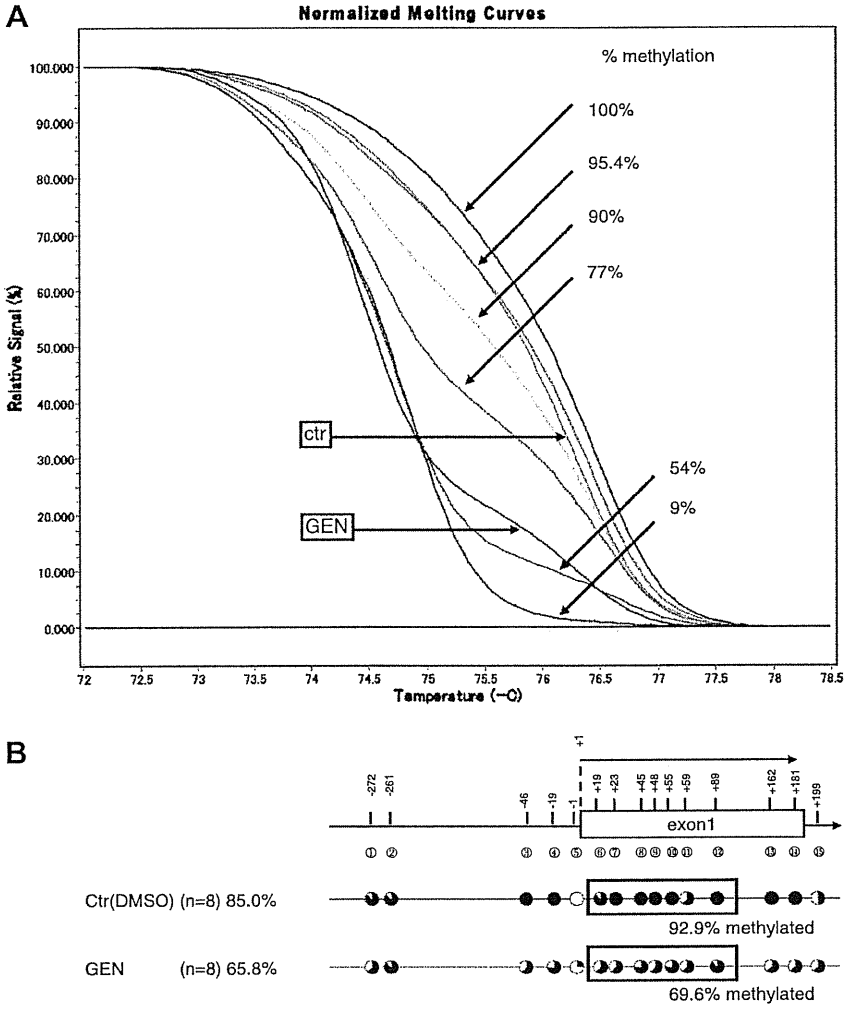

Fig. 4. Genistein induced demethylation of the SF-1 gene in the cell clone that showed the highest proliferative activity. (A) The GEN-mediated demethylation of CpGs (at the positions of +19, 23, 45, 48, 55, 59, and 89) in the SF-1 gene *in vitro* in one out of 20 isolated clones (Fig. 3A and C). HRM analysis enabled to clear separation of the PCR product mixtures with different CpG compositions. The methylation standards were prepared as 100% (red), 95.4% (orange), 90% (yellow), 77% (green), 54% (blue), and 9% (violet) methylated template in demethylated background. Grey and pink indicate the control and GEN-treated clone sample, respectively. (B) SF-1 DNA methylation status, obtained from bisulfate sequencing, of the clone that showed demethylation in HRM assay. Percentage under box (HRM region) indicates percent methylation of HRM region. (For interpretation of the references to color in this figure legend, the reader is referred to the web version of this paper.)

CpG sites in the SF-1 promoter (Fig. 2), and substantial increase in SF-1 mRNA level (Fig. 1B). Expressions of genes downstream of transcription factor SF-1 were also significantly enhanced (Fig. 1C–F). However, it should be noted that the induced mRNA levels were still very low (Fig. 1B–F), less than one copy per cell, as determined by the Percellome method [16]. Our results are consistent with those of a previous study reporting that a physiological concentration of GEN increased Cyp19a1 enzymatic activity in endometrial cells derived from a normal uterus, whereas GEN did not affect Cyp19a1 activity in a cell-free assay [24]. It is unknown whether GEN stimulated Cyp19a1 activity by epigenetic modulation.

In the present study, we also identified primary cultured endometrial cells that were competent for epigenetic regulation by GEN, which were present at a very low frequency. In our *in vitro* study, GEN treatment did not enhance, but rather inhibited the proliferation of colony-derived cells. Taken together, these findings indicate that a minor population of endometrium cells can respond to GEN and that, in these cells, GEN induces demethylation and activation of SF-1, followed by the induction of the SF-1 steroidogenic cascade. This might lead to local steroidogenesis and enhanced endometrium proliferation *in vivo* in GEN-treated OVX mice. Since demethylation of the SF-1 promoter was observed at the whole tissue level (Fig. 2), and the induced expression of steroidogenic genes occurred only to a subcellular amount (Fig. 1B–F), the demethylation event in each cell may not be sufficient for the SF-1 induction.

The demethylation in the endometrium that occurred after 1 week of treatment with high-dose GEN was more prominent in the LU than in the MY. Following GEN treatment, the methylation level in the MY was similar to that in the untreated endometrium as a whole. After 7 days of GEN exposure, the endometrial cells in the LU of OVX mice were composed of regenerated cells moving from MY to LU; in light of this, our results indicate that the initial epigenetic alteration might be expanded through proliferation of regenerating cells. This is also consistent with our observation that more endometrial cells derived from MY showed higher colony-formation activity and rapid proliferation than did those derived

from LU (Fig. 3). We thus speculate that there are GEN-sensitive cells in the MY, which might contain endometrial stem cells [25].

Recently, human endometrial stem cells were identified; they reside in endometrial stromal tissue and possess fibroblastic-shape and self-renewal ability, thus forming large, densely packed, homogenous colonies [17,18]. Some candidates for murine endometrial progenitor cells have been suggested to reside in the luminal epithelial or area of adjacent to the myometrium [25]. The rapidly growing endometrial cell that we obtained had a fibroblastic-shape, formed large, relatively homogenous, densely packed colonies, and showed self-renewal activity when seeded at a very low cell density (data not shown). Although there are differences between the species, we speculate that our rapid growing cell clones may correspond to the human endometrial stromal progenitors cells [17].

Aberrant SF-1 expression with lack of promoter CpG methylation has been reported in ectopic endometriosis [14], and thus endometriosis is now considered an epigenetic disease [26]. Endometriosis is classically defined as the growth of endometrial tissue at extrauterine sites; it has been suggested that each endometriotic lesion originates from a single epigenetically deregulated endometrial progenitor cell [27]. Further studies are required to identify cells which are competent for epigenetic changes following GEN exposure, and to elucidate the relationships between these cells, GEN, and endometriosis.

In conclusion, we demonstrated that GEN demethylates the promoter region of the SF-1 gene. This is the first demonstration of phytoestrogen participation in epigenetic alterations in adult endometrial tissue. These findings are important from standpoints of nutrition, public health, and disease prevention. Further study is warranted to characterize the nature of the cells that respond to GEN in the endometrium.

Appendix A. Supplementary data

Supplementary data associated with this article can be found, in the online version, at doi:10.1016/j.bbrc.2011.07.104.

References

[1] H. Adlercreutz, Phyto-oestrogens and cancer, Lancet Oncol. 3 (2002) 364–373.
[2] M. Messina, W. McCaskill-Stevens, J.W. Lampe, Addressing the soy and breast cancer relationship: review, commentary, and workshop proceedings, J. Natl. Cancer Inst. 98 (2006) 1275–1284.
[3] A.H. Wu, R.G. Ziegler, A.M. Nomura, D.W. West, L.N. Kolonel, P.L. Horn-Ross, R.N. Hoover, M.C. Pike, Soy intake and risk of breast cancer in Asians and Asian Americans, Am. J. Clin. Nutr. 68 (1998) 1437S–1443S.
[4] J. Kanno, L. Onyon, S. Peddada, J. Ashby, E. Jacob, W. Owens, The OECD program to validate the rat uterotrophic bioassay. Phase 2: dose–response studies, Environ. Health Perspect. 111 (2003) 1530–1549.
[5] K. Pettersson, J.A. Gustafsson, Role of estrogen receptor beta in estrogen action, Annu. Rev. Physiol. 63 (2001) 165–192.
[6] P. Diel, T. Hertrampf, J. Seibel, U. Laudenbach-Leschowsky, S. Kolba, G. Vollmer, Combinatorial effects of the phytoestrogen genistein and of estradiol in uterus and liver of female Wistar rats, J. Steroid Biochem. Mol. Biol. 102 (2006) 60–70.
[7] V. Beck, U. Rohr, A. Jungbauer, Phytoestrogens derived from red clover: an alternative to estrogen replacement therapy?, J Steroid Biochem. Mol. Biol. 94 (2005) 499–518.
[8] N. Sato, N. Yamakawa, M. Masuda, K. Sudo, I. Hatada, M. Muramatsu, Genome-wide DNA methylation analysis reveals phytoestrogen modification of promoter methylation patterns during embryonic stem cell differentiation, PLoS One 6 (2011) e19278.
[9] S.M. Meeran, A. Ahmed, T.O. Tollefsbol, Epigenetic targets of bioactive dietary components for cancer prevention and therapy, Clin. Epigenetics 1 (2010) 101–116.
[10] S. Majid, A.A. Dar, V. Shahryari, H. Hirata, A. Ahmad, S. Saini, Y. Tanaka, A.V. Dahiya, R. Dahiya, Genistein reverses hypermethylation and induces active histone modifications in tumor suppressor gene B-Cell translocation gene 3 in prostate cancer, Cancer 116 (2010) 66–76.
[11] A.K. Jha, M. Nikbakht, G. Parashar, A. Shrivastava, N. Capalash, J. Kaur, Reversal of hypermethylation and reactivation of the RARbeta2 gene by natural compounds in cervical cancer cell lines, Folia. Biol. (Praha) 56 (2010) 195–200.
[12] Y. Li, T.O. Tollefsbol, Impact on DNA methylation in cancer prevention and therapy by bioactive dietary components, Curr. Med. Chem. 17 (2010) 2141–2151.
[13] K. Morohashi, S. Honda, Y. Inomata, H. Handa, T. Omura, A common trans-acting factor, Ad4-binding protein, to the promoters of steroidogenic P-450s, J. Biol. Chem. 267 (1992) 17913–17919.
[14] Q. Xue, Z. Lin, P. Yin, M.P. Milad, Y.H. Cheng, E. Confino, S. Reierstad, S.E. Bulun, Transcriptional activation of steroidogenic factor-1 by hypomethylation of the 5′ CpG island in endometriosis, J. Clin. Endocrinol. Metab. 92 (2007) 3261–3267.
[15] S.E. Bulun, H. Utsunomiya, Z. Lin, P. Yin, Y.H. Cheng, M.E. Pavone, H. Tokunaga, E. Trukhacheva, E. Attar, B. Gurates, M.P. Milad, E. Confino, E. Su, S. Reierstad, Q. Xue, Steroidogenic factor-1 and endometriosis, Mol. Cell. Endocrinol. 300 (2009) 104–108.
[16] J. Kanno, K. Aisaki, K. Igarashi, N. Nakatsu, A. Ono, Y. Kodama, T. Nagao, "Per cell" normalization method for mRNA measurement by quantitative PCR and microarrays, BMC Genomics 7 (2006) 64.
[17] R.W. Chan, K.E. Schwab, C.E. Gargett, Clonogenicity of human endometrial epithelial and stromal cells, Biol. Reprod. 70 (2004) 1738–1750.
[18] C.E. Gargett, K.E. Schwab, R.M. Zillwood, H.P. Nguyen, D. Wu, Isolation and culture of epithelial progenitors and mesenchymal stem cells from human endometrium, Biol. Reprod. 80 (2009) 1136–1145.
[19] Y. Kumaki, M. Oda, M. Okano, QUMA: quantification tool for methylation analysis, Nucleic Acids Res. 36 (2008) W170–W175.
[20] J.A. McKay, J.C. Mathers, Diet induced epigenetic changes and their implications for health, Acta Physiol. (Oxf) (2011) 103–118.
[21] B.C. Christensen, E.A. Houseman, C.J. Marsit, S. Zheng, M.R. Wrensch, J.L. Wiemels, H.H. Nelson, M.R. Karagas, J.F. Padbury, R. Bueno, D.J. Sugarbaker, R.F. Yeh, J.K. Wiencke, K.T. Kelsey, Aging and environmental exposures alter tissue-specific DNA methylation dependent upon CpG island context, PLoS Genet. 5 (2009) e1000602.
[22] C.B. Klein, A.A. King, Genistein genotoxicity: critical considerations of in vitro exposure dose, Toxicol. Appl. Pharmacol. 224 (2007) 1–11.
[23] G. Rimoldi, J. Christoffel, D. Seidlova-Wuttke, H. Jarry, W. Wuttke, Effects of chronic genistein treatment in mammary gland, uterus, and vagina, Environ. Health Perspect. 115 (Suppl. 1) (2007) 62–68.
[24] K.M. Edmunds, A.C. Holloway, D.J. Crankshaw, S.K. Agarwal, W.G. Foster, The effects of dietary phytoestrogens on aromatase activity in human endometrial stromal cells, Reprod. Nutr. Dev. 45 (2005) 709–720.
[25] C.E. Gargett, H. Masuda, Adult stem cells in the endometrium, Mol. Hum. Reprod. 16 (2010) 818–834.
[26] S.W. Guo, Epigenetics of endometriosis, Mol. Hum. Reprod. 15 (2009) 587–607.
[27] Y. Wu, Z. Basir, A. Kajdacsy-Balla, E. Strawn, V. Macias, K. Montgomery, S.W. Guo, Resolution of clonal origins for endometriotic lesions using laser capture microdissection and the human androgen receptor (HUMARA) assay, Fertil. Steril. 79 (Suppl. 1) (2003) 710–717.

nature cell biology

PKA-dependent regulation of the histone lysine demethylase complex PHF2–ARID5B

Atsushi Baba[1], Fumiaki Ohtake[1,2], Yosuke Okuno[1,2], Kenichi Yokota[1], Maiko Okada[1,2], Yuuki Imai[1,3], Min Ni[3], Clifford A. Meyer[4], Katsuhide Igarashi[5], Jun Kanno[5], Myles Brown[3] and Shigeaki Kato[1,2,6]

Reversible histone methylation and demethylation are highly regulated processes that are crucial for chromatin reorganization and regulation of gene transcription in response to extracellular conditions. However, the mechanisms that regulate histone-modifying enzymes are largely unknown. Here, we characterized a protein kinase A (PKA)-dependent histone lysine demethylase complex, PHF2–ARID5B. PHF2, a jmjC demethylase, is enzymatically inactive by itself, but becomes an active H3K9Me2 demethylase through PKA-mediated phosphorylation. We found that phosphorylated PHF2 then associates with ARID5B, a DNA-binding protein, and induce demethylation of methylated ARID5B. This modification leads to targeting of the PHF2–ARID5B complex to its target promoters, where it removes the repressive H3K9Me2 mark. These findings suggest that the PHF2–ARID5B complex is a signal-sensing modulator of histone methylation and gene transcription, in which phosphorylation of PHF2 enables subsequent formation of a competent and specific histone demethylase complex.

Post-translational modifications of histone amino-terminal tails, including reversible acetylation, methylation, phosphorylation and ubiquitylation, modulate both chromatin structure and gene regulation[1,2]. Reversible histone methylation defines the state of chromatin; repressive histone methylation marks such as H3K9Me2 inhibit gene transcription from nearby promoters, and removal of these marks by histone lysine demethylases permit transcription. Thus, enzymes such as jmjC (Jumonji C)-domain-containing histone lysine demethylases seem to play pivotal roles in epigenetic control[3–10]. Though histone marks are altered in response to extracellular signals, the underlying mechanism by which this is achieved is largely unknown.

RESULTS

Identification of the PHF2–ARID5B histone H3K9Me2 demethylase complex

During biochemical identification of transcriptional co-regulators for nuclear receptors[11,12], we purified a number of direct interactants for nuclear receptors. Among them, a co-activator complex for FXR (farnesoid X receptor) from HepG2 cells was selected for further analysis, because its abundance in the purified fractions was significantly increased when the cells were pretreated with forskolin (FSK), a protein kinase A (PKA) activator (Supplementary Fig. S1a). Matrix-assisted laser desorption/ionization–time of flight mass spectrometry analysis of the purified complex[11,12] identified three subunits: plant homeodomain (PHD) finger two (PHF2; ref. 13), AT-rich interactive domain 5B (ARID5B) isoform α and ARID5B isoform β (ref. 14; Fig. 1a and Supplementary Fig. S1b–e). The complex was still detectable after further column purification (Supplementary Fig. S1f). ARID5B contains the ARID/Bright domain, which is seen in subunits of chromatin-remodelling complexes and is considered to be a sequence-specific/nonspecific DNA-attachment domain[14]. PHF2 (ref. 13) contains PHD and jmjC domains[4,6]. Unlike several other jmjC histone demethylases[3,5,8,9], PHF2 lacks the ARID domain. PHF2 and ARID5B genes are expressed in a broad range of tissues, including liver (Supplementary Fig. S2c), and at protein levels as well in various cell lines (Supplementary Fig. S2a,b,d). PHF2 physically interacted with FXR and HNF4α (hepatocyte nuclear factor 4α; Supplementary Fig. S3a,b,d), but not with ERα (oestrogen receptor alpha) or VDR (vitamin D receptor; Supplementary Fig. S3c,d). PHF2 directly interacted with ARID5B *in vitro* (Supplementary Fig. S3e–g).

The PHF2–ARID5B complex was purified from HepG2 cells stably expressing Flag–PHF2. As jmjC-domain-containing proteins catalyse lysine demethylation[3–10], we investigated the histone lysine demethylation activity of the purified PHF2 complex[7,10]. The PHF2 complex exhibited lysine demethylase activity *in vitro* as assessed by a formaldehyde release (Fig. 1b). Then we examined

[1]Institute of Molecular and Cellular Biosciences, University of Tokyo, 1-1-1 Yayoi, Bunkyo-ku, Tokyo 113-0032, Japan. [2]ERATO, Japan Science and Technology Agency, 4-1-8 Honcho, Kawaguchishi, Saitama 332-0012, Japan. [3]Department of Medical Oncology, Dana-Farber Cancer Institute and Harvard Medical School, Boston, Massachusetts 02115, USA. [4]Department of Biostatistics and Computational Biology, Dana-Farber Cancer Institute and Harvard School of Public Health, Boston, Massachusetts 02115, USA. [5]Division of Cellular and Molecular Toxicology, National Institute of Health Sciences, 1-18-1 Kamiyoga, Setagaya-ku, Tokyo 158-8501, Japan.
[6]Correspondence should be addressed to S.K. (e-mail: uskato@mail.ecc.u-tokyo.ac.jp)

Received 14 July 2011; accepted 28 February 2011; published online 1 May 2011; DOI: 10.1038/ncb2228

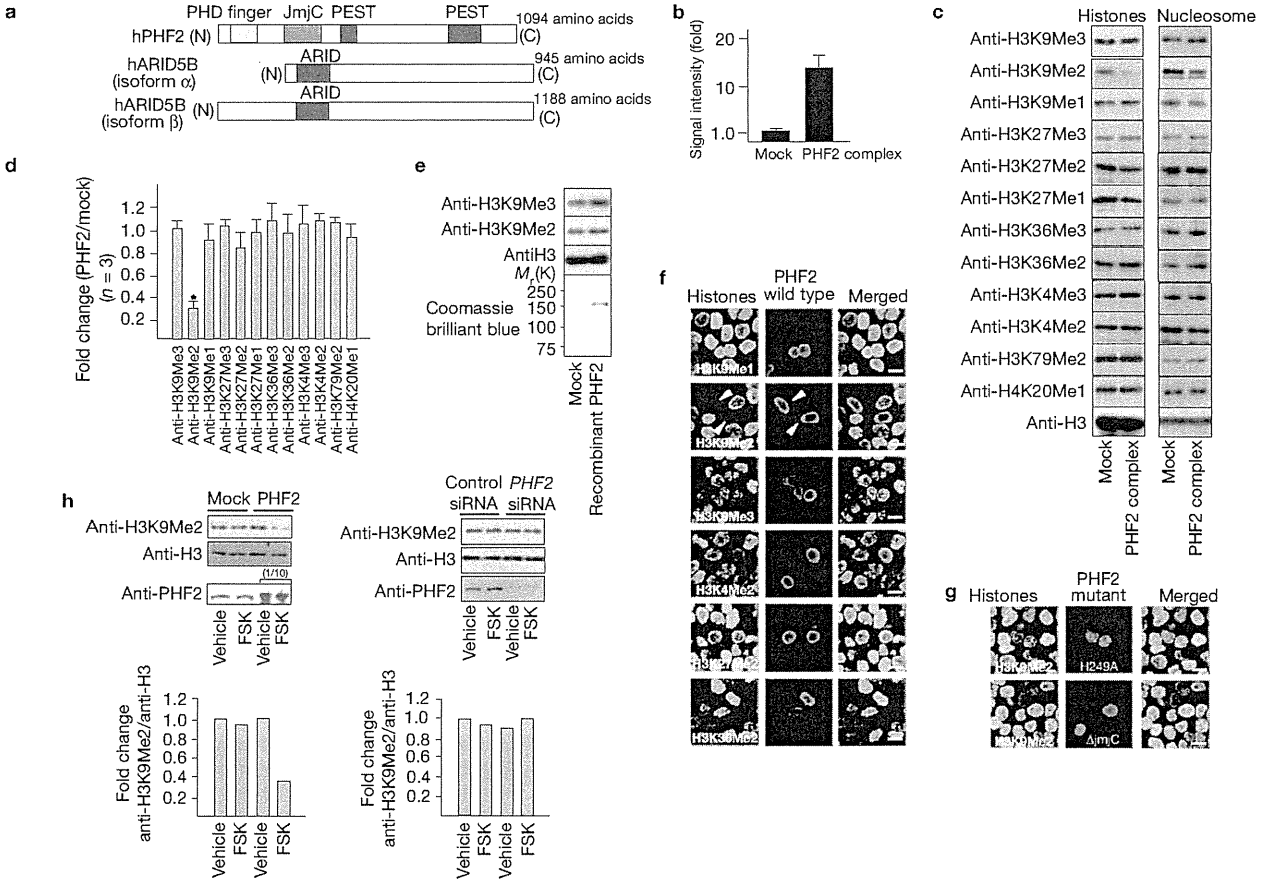

Figure 1 Identification of the PHF2–ARID5B histone H3K9Me2 demethylase complex. (**a**) A schematic representation of domains of PHF2 and ARID5B. (**b–d**) Histone H3K9Me2 demethylase activity of the purified PHF2 complex *in vitro*. (**b**) Native histones were incubated with PHF2 complex, and formaldehyde release was analysed by fluorescence detection. Shown is the average ± s.d. ($n = 3$) of the relative activity. (**c**) The PHF2 complex was incubated with purified native histones (left) or mononucleosomes (right) for demethylation reaction, and each modification was determined by western blotting as indicated. (**d**) Intensity of histone marks in the demethylation assay of native histones by PHF2 (in **c** and Supplementary Fig. S8a) was quantified, and averages ± s.d. of three independent experiments are shown. The asterisk shows $P < 0.05$ in Student's t-test. (**e**) Recombinant PHF2 protein is catalytically inactive. Recombinant PHF2 protein (lower panel) was subjected to *in vitro* demethylation assay (upper panels). (**f**) 293F cells were transfected with Flag–PHF2 expression vectors for 24 h and treated with FSK for 6 h, then cells were fixed and immunostained with the indicated antibodies. Note the decreased level of H3K9Me2 in the anti-Flag-positive cells (arrowheads). Scale bars, 40 μm. (**g**) 293F cells were transfected with either the Flag–PHF2$^{\Delta jmjC}$ or the HA–PHF2^{H249A} mutant, and immunostaining was carried out as in **f**. Scale bars, 40 μm. (**h**) H3K9Me2 demethylation activity of PHF2 *in vivo*. 293F cells transfected with the indicated expression vectors or short interfering RNAs (siRNAs), and were treated with FSK for 6 h. The soluble chromatin fraction was subjected to western blotting as indicated. Uncropped images of blots are shown in Supplementary Fig. S9.

the site-specificity of lysine demethylation using native histones or purified mononucleosomes as substrates. *In vitro*, the PHF2 complex demethylated dimethylated Lys 9 on histone H3 (H3K9Me2), but neither mono- nor trimethylated H3K9 (H3K9Me1, Me3) (Fig. 1c,d). Methylated H3K4, K27, K36 and K79 and H4K20 seemed unlikely PHF2 substrates (Fig. 1c,d). Thus it is likely that PHF2 substrate recognition is more specific than the closely related PHF subfamily members such as PHF8 and KDM7/KIAA1718 (refs 15–17). This demethylase activity was not detected in recombinant PHF2 protein (Fig. 1e). PHF2 did not demethylate a methylated peptide (amino acids 1–21 of H3) containing K9Me2 (Supplementary Fig. S4a). Such substrate specificity is known for Lid2 (ref. 18) and yeast Lsd1 (ref. 19), and possibly due to requirement of other regions of H3. Immunostaining analysis of 293F cells confirmed that PHF2 almost entirely demethylated H3K9Me2 in the presence of FSK, but had only marginal effects on H3K27Me2 and the other tested methylated histones (Fig. 1f and Supplementary Fig. S4b). The conserved histidine residue within the PHF2 jmjC domain was required for enzymatic activity (Fig. 1g). In 293F cells, overexpression of PHF2 in the presence of FSK decreased H3K9Me2, whereas knockdown of PHF2 did not lead to global increase of this mark (Fig. 1h), raising the possibility that other H3K9 demethylase(s) may compensate for PHF2 in these cells.

PHF2 is phosphorylated by PKA at a specific serine residue

In a co-immunoprecipitation assay, association of PHF2 and ARID5B was inducible on FSK treatment of immortalized hepatocytes[20] both in the absence (Fig. 2a) and presence (Supplementary Fig. S4c) of a proteasomal inhibitor, MG132. Consistently, abundance of these proteins was not clearly affected by FSK treatment (Supplementary Fig. S4d). Therefore, we reasoned that phosphorylation of the factor(s) by PKA was a trigger to induce association. Endogenous PHF2, but not ARID5B, was phosphorylated by FSK treatment of the cells (Fig. 2b,c).

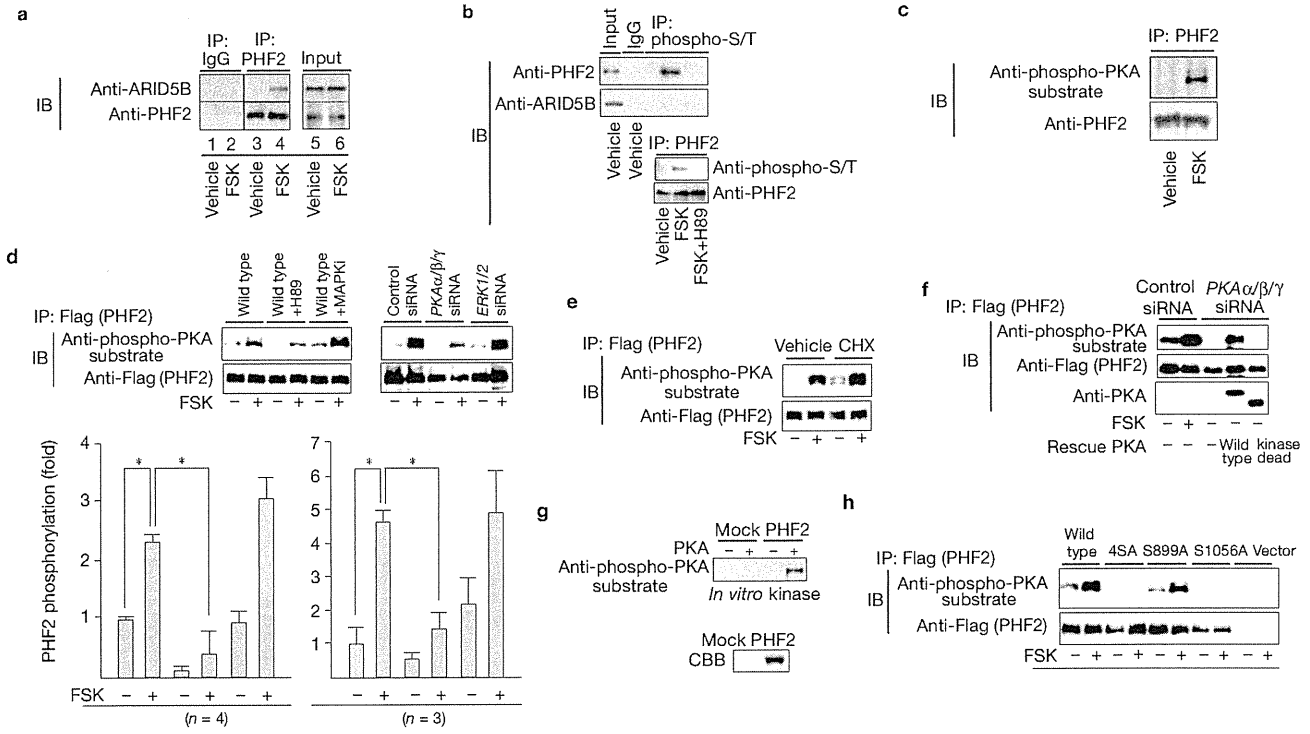

Figure 2 PKA-dependent complex assembly of PHF2–ARID5B. (**a**) Assembly of the endogenous PHF2–ARID5B complex. Hepatocytes were treated with the indicated compounds for 2 h and were subjected to immunoprecipitation (IP) and immunoblotting (IB) with the indicated antibodies. Specificity of antibodies was confirmed in Supplementary Fig. S2a,b. (**b**,**c**) Phosphorylation of endogenous PHF2 by PKA. Hepatocytes (**b**) or 293F cells (**c**) were treated with vehicle, FSK, or FSK +H89 as indicated for 2 h, then lysates were immunoprecipitated using either anti-phospho-serine/threonine or anti-PHF2 antibodies. The eluates were subjected to western blotting as indicated. (**d**–**f**) 293F cells transfected with Flag–PHF2 and indicated siRNAs were treated with the indicated inhibitors, and immunoprecipitated with anti-Flag antibodies. Immunoprecipitates were subjected to immunoblotting with an anti-phospho-PKA substrate antibody. (**d**, lower panel) Averages ± s.d. The other data sets are shown in Supplementary Fig. S8b,c. The asterisks show $P < 0.05$ in Student's *t*-test. (**g**) *In vitro* kinase assay with recombinant PHF2 and PKA proteins. (**h**) PHF2 is phosphorylated by PKA at Ser 757/899/954/1056. In the 4SA mutants, Ser 757/899/954/1056 were replaced with alanines. Uncropped images of blots are shown in Supplementary Fig. S9.

FSK-dependent PHF2 phosphorylation was negated by the PKA inhibitor H89, but not by a MAP kinase inhibitor (MAPKi; Fig. 2d). Cyclohexamide (CHX) did not attenuate PHF2 phosphorylation, indicating that this event does not mediate *de novo* protein synthesis (Fig. 2e). Knockdown of PKAα/β/γ, but not of extracellular signal-regulated kinases ERK1/2, abrogated PHF2 phosphorylation (Fig. 2d,f and Supplementary Fig. S5a). PKA phosphorylated recombinant PHF2 in *in vitro* phosphorylation assays (Fig. 2g). Using recombinant PHF2 deletion mutants, the carboxy-terminal region of PHF2 was mapped to be phosphorylated by PKA (Supplementary Fig. S5b,d), and bears four conserved, PKA consensus serine residues (Supplementary Fig. S5c). Replacement of all of four serine residues by alanines (4SA: Ser 757/Ser 899/Ser 954/Ser 1056) fully abrogated PKA phosphorylation of PHF2 (Fig. 2h). Further mapping revealed that Ser 1056 seemed to be a major phosphorylation site (Fig. 2h).

PKA-dependent demethylase activity of PHF2–ARID5B complex

We then asked if the demethylase activity of PHF2 for H3K9Me2 was also PKA dependent with proteins purified from 293F cells as well as recombinant proteins. Purified PHF2 protein, phosphorylated by PKA *in vitro*, exhibited H3K9Me2 demethylase activity (Fig. 3a–c). Conversely, PHF2 phosphorylated by FSK treatment in cells exhibited the demethylase activity, but *in vitro* dephosphorylation by BAP (bacterial alkaline phosphatase) negated the demethylase activity (Fig. 3b,c). ARID5B was dispensable for the enzymatic activity of PHF2 *in vitro* (Fig. 3b,c), because ARID5B was absent from the purified PHF2 protein fraction used (Supplementary Fig. S5f). Similarly, recombinant PHF2 was activated by PKA phosphorylation (Fig. 3d–f). PHF2 phosphorylation mutants were not activated by PKA (Fig. 3g). Consistent with the *in vitro* analyses, H3K9Me2 demethylation by overexpression of PHF2–ARID5B in cells was significantly enhanced by FSK treatment, but 4SA was not activated by FSK (Fig. 3h). Subnuclear localization patterns of the $PHF2^{4SA}$ mutant did not look identical to that of wild-type PHF2 (Fig. 3h), raising the possibility that PHF2 phosphorylation is indispensable for chromatin association. Together, these findings suggest that PKA-mediated phosphorylation induces the demethylase activity of PHF2, unlike the other characterized jmjC demethylases exhibiting constitutive enzymatic activities both *in vivo* and *in vitro* as recombinant proteins[4–10].

ARID5B directs PKA-dependent promoter targeting of PHF2

We examined how PKA-mediated activation of the PHF2–ARID5B complex activated transcription at endogenous promoters. In immortalized hepatocytes, glucagon–PKA signalling regulates glucose

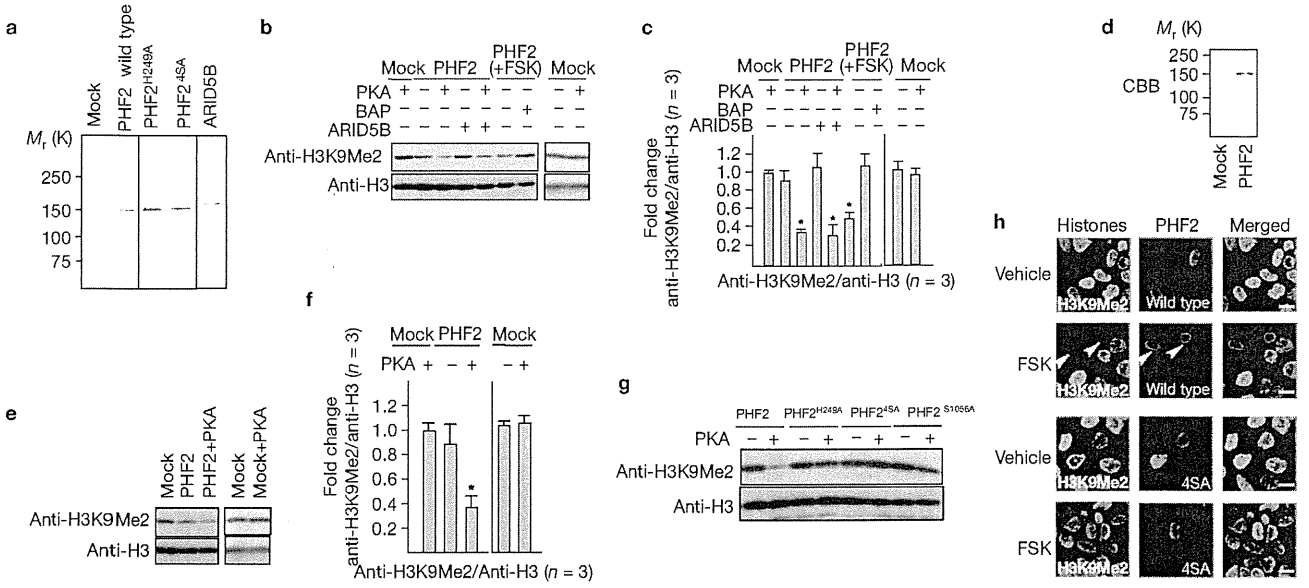

Figure 3 PKA-dependent demethylase activity of the PHF2–ARID5B complex. (**a**) The indicated proteins were purified to near homogeneity from 293F cells. Purification of PHF2 mutants is shown in Supplementary Fig. S5e. Note that purified PHF2 did not include ARID5B (Supplementary Fig. S5f). (**b**,**c**) *In vitro* histone demethylation assay. Purified PHF2 protein or PHF2 mutants were incubated with either PKA or BAP as indicated, and *in vitro* demethylation assays were carried out with/without purified ARID5B protein. (**c**) The signal intensity of three independent experiments (performed as in **b** and Supplementary Fig. S8d) was quantified. Data are averages ± s.d. The asterisks show $P < 0.05$ in Student's *t*-test. (**d**–**f**) Recombinant PHF2 protein purified to near homogeneity from Sf9 cells was phosphorylated by PKA, and *in vitro* demethylation assay was carried out as in **b**,**c**. (**f**) Data are averages ± s.d. ($n = 3$, Supplementary Fig. S8e). The asterisk shows $P < 0.05$ in Student's *t*-test. (**g**) *In vitro* histone demethylation assay as in **b** with the indicated PHF2 mutants. (**h**) H3K9Me2 demethylation activity of PHF2–ARID5B is FSK dependent *in vivo*. 293F cells transfected with wild-type or $PHF2^{4SA}$ were treated with FSK for 6 h. Scale bars, 40 μm. Uncropped images of blots are shown in Supplementary Fig. S9.

homeostasis through induction of gluconeogenic enzymes, such as Pepck and G6Pase (refs 20–23). Chromatin immunoprecipitation (ChIP) analysis revealed glucagon–PKA-induced promoter binding of PHF2–ARID5B at the promoters of *Pepck* and *G6Pase* (Fig. 4a). Sequential ChIP (Re-ChIP) suggested that the endogenous PHF2–ARID5B complex associates with the *Pepck* promoter (Fig. 4b), without protein synthesis (Fig. 4b and Supplementary Fig. S6a). H89 abrogated glucagon-mediated recruitment of these factors (Supplementary Fig. S6b). PHF2 and ARID5B were co-recruited to *Pepck* promoter on similar time-courses (Supplementary Fig. S6c). Demethylation of H3K9Me2 was induced by FSK, coupled with PHF2 recruitment (Fig. 4a and Supplementary Fig. S6c). However, the H3K9Me1 level was not significantly altered by FSK treatment (Fig. 4a), suggesting that newly produced H3K9Me1 was sequentially demethylated by other H3K9 demethylase(s). H3K9Me3 signal was low in both the presence and absence of FSK (Fig. 4a), consistent with the notion that *Pepck* and *G6Pase* gene promoters are converted to euchromatin in hepatocytes.

We further explored the mechanism for PKA-dependent promoter recruitment of PHF2–ARID5B. Although ARID5B was dispensable for PHF2 enzymatic activity *in vitro* (Fig. 3b), ARID5B was required for promoter targeting of PHF2 and H3K9Me2 demethylation *in vivo* (Fig. 4c, lanes 9–12, 4d). Knockdown of PHF2 by RNA interference attenuated FSK-induced recruitment of ARID5B to the promoters (Fig. 4c, lanes 3–4, 4d), indicating the signal-sensing role of PHF2 in directing the complex to target promoters. A specific PHF2 mutant (H249A), lacking a conserved histidine essential for its lysine demethylation activity (Fig. 1g), was unable to anchor PHF2–ARID5B on the target gene promoter (Fig. 4c, lanes 7, 8). We reasoned that a lysine demethylation event occurred before chromatin association. Therefore, we determined whether ARID5B was a substrate for the PHF2 demethylase. Exogenously expressed ARID5B was lysine-methylated in hepatocytes in the absence of FSK (Fig. 5a, lane 2). PHF2 induced demethylation of ARID5B in the presence of FSK through the jmjC domain (Fig. 5a, lanes 3–4). ARID5B, but not other ARID family proteins, harbours a lysine motif (Lys 336) in the ARID domain that resembles the alignment around histone H3K9 (Supplementary Fig. S6d). When Lys 336 of ARID5B was replaced by alanine (K336A), the methylated form of ARID5B was no longer detected (Fig. 5a, lane 5). An anti-ARID5B-K336Me2 antibody was raised, and the specificity was confirmed by an enzyme-linked immunosorbent assay with methylated ARID5B (Supplementary Fig. S6e) as well as with unmethylated K336A or K336R mutants (Fig. 5b). We found that PHF2 promoted demethylation of ARID5B at Lys 336 (Fig. 5c). Catalytically inactive $PHF2^{H249A}$ increased the ARID5B K336Me2 mark (Fig. 5c), and endogenous ARID5B was demethylated following FSK treatment (Fig. 5d). Moreover, purified PHF2 protein demethylated ARID5B at Lys 336 *in vitro* (Fig. 5e). We then used a DNA pulldown (ABCD) assay to determine if demethylation of Lys 336-methylated ARID5B converted it to an active form on DNA binding. Only when cells were treated with FSK, ARID5B–PHF2 complex was recruited to synthetic oligonucleotides containing the *Pepck* promoter sequences[24,25] (Fig. 5f). FSK-dependent DNA binding of PHF2–ARID5B was abolished in $PHF2^{H249A}$ and $ARID5B^{K336A}$ mutants (Fig. 5f). Neither $PHF2^{H249A}$ nor $ARID5B^{K336A}$ supported FSK-mediated promoter recruitment and subsequent H3K9Me2 demethylation (Fig. 4c).

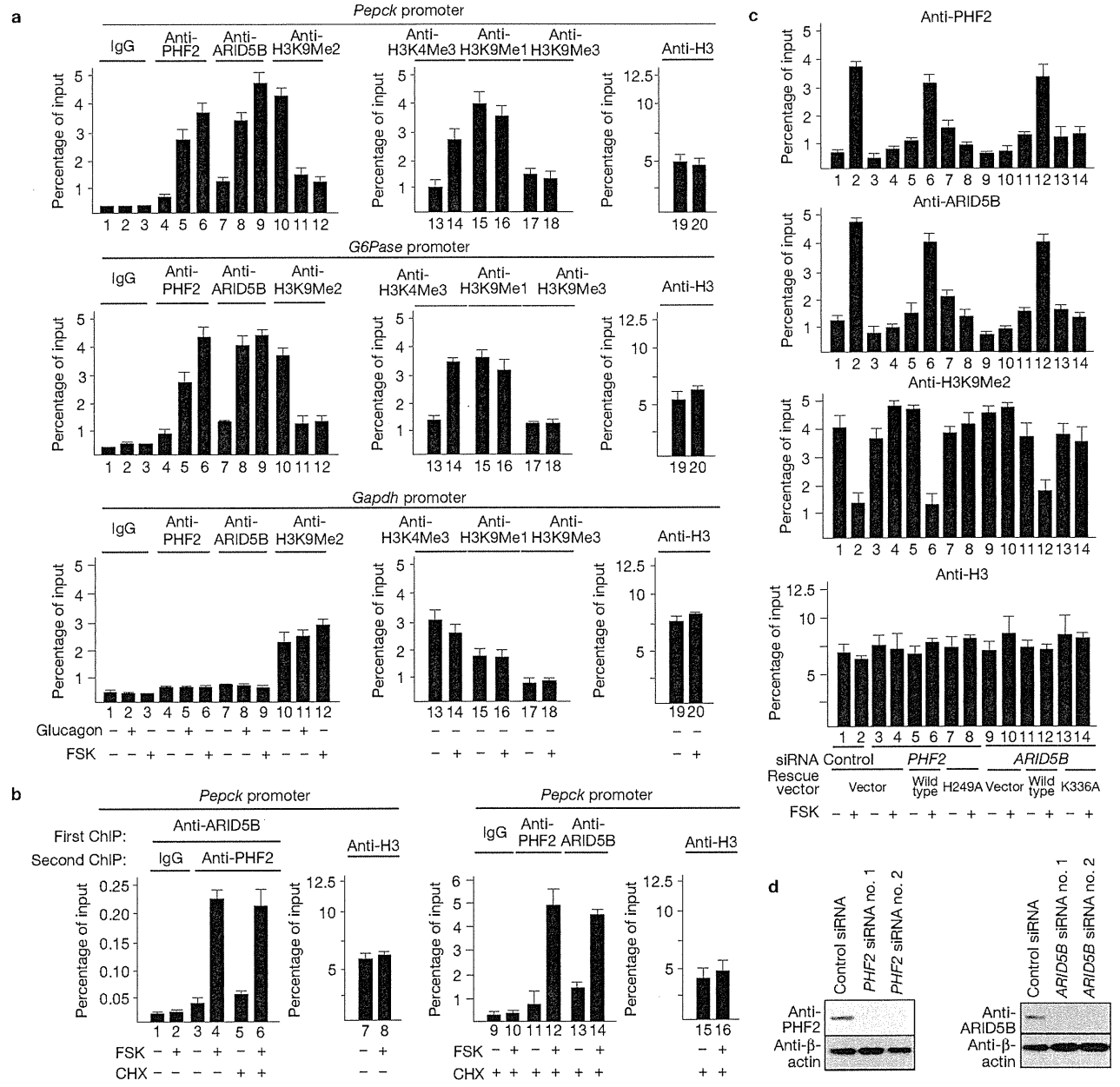

Figure 4 PKA-dependent promoter targeting of PHF2–ARID5B. (**a**) Endogenous PHF2–ARID5B complex is recruited to the promoter regions of *Pepck* and *G6Pase*, but not to that of *Gapdh*, in a glucagon–PKA-dependent manner. Hepatocytes were treated with the indicated compounds for 4 h, and ChIP assays were carried out using indicated antibodies. Data are average ± s.d. ($n = 3$). (**b**) ChIP and Re-ChIP assays. Hepatocytes were treated with the indicated compounds for 4 h, then sequentially immunoprecipitated with the indicated antibodies. Data are average ± s.d. ($n = 3$). (**c**) Promoter targeting and H3K9Me2 demethylase activities of PHF2–ARID5B mutants in ChIP assays. Hepatocytes were transfected with the indicated siRNAs for 24 h, then with the indicated rescue vector for a further 12 h. Then, cells were treated with FSK for 4 h and ChIP assays were carried out. Data are average ± s.d. ($n = 3$). (**d**) The knockdown efficiencies of siRNAs in immortalized hepatocytes were determined using samples in **c**. Uncropped images of blots are shown in Supplementary Fig. S9.

PHF2–ARID5B acts as a co-activator for HNF4α in liver of fasted mice

The transcriptional effects mediated by PHF2–ARID5B were assessed by monitoring gene expression in hepatocytes. PKA-dependent gene induction of *Pepck* and *G6Pase* was impaired (Fig. 6a) following knockdown of PHF2 or ARID5B in hepatocytes (Fig. 4d). The unphosphorylated PHF2 mutant ($PHF2^{4SA}$) was unable to confer the FSK response (Fig. 6a). As HNF4α is activated by the glucagon–PKA signalling pathway and serves as the primary transcriptional activator on *Pepck* and *G6Pase* promoters[21,22,26–28], we further characterized the transcriptional co-activation function of PHF2–ARID5B towards HNF4α. In a luciferase reporter assay in the presence of FSK (refs 12,29), PHF2 acted as a co-activator for HNF4α (Fig. 6b) as well as FXR (Supplementary Fig. S7) in 293F

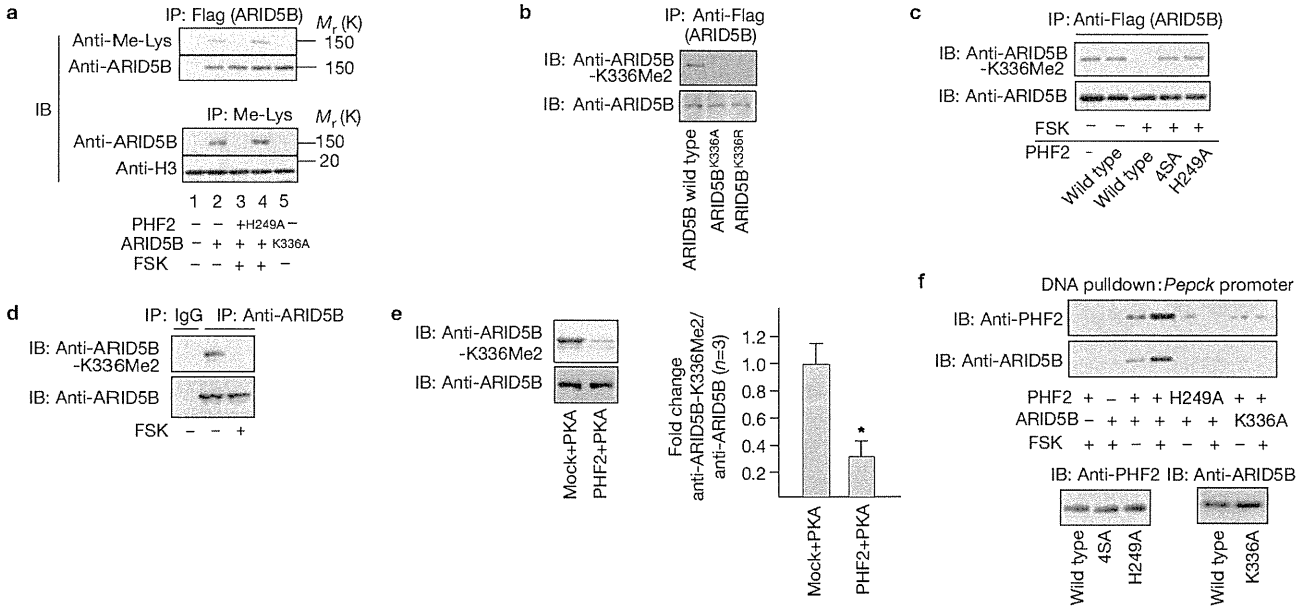

Figure 5 ARID5B directs PKA-dependent promoter targeting of PHF2. (**a**) PHF2 induces demethylation of ARID5B. The methylation state of ARID5B in 293F cells was examined using anti-ARID5B and anti-methyl-lysine antibodies. Wild-type, but not K336A, ARID5B is a lysine-methylated protein. (**b**) Confirmation of specificity of anti-ARID5B-K336Me2 antibody. 293F cells were transfected with the indicated ARID5B mutants and immunoprecipitated/blotted with the indicated antibodies. (**c**) Demethylation of ARID5B is dependent on the catalytic activity of PHF2 in hepatocytes as revealed by the specified anti-ARID5B-K336Me2 antibody. (**d**) Lys 336 methylation of endogenous ARID5B. 293F cells were treated with FSK for 4 h, then immunoprecipitation was carried out as indicated. (**e**) *In vitro* ARID5B demethylation assay. Flag–ARID5B purified from 293F cells was incubated with purified PHF2 (Fig. 3a), and the demethylation was detected by western blotting. The signal intensity of three independent experiments (in the upper panel and in Supplementary Fig. S8f) was quantified. Data are averages ± s.d. ($n = 3$). The asterisk shows $P < 0.05$ in Student's t-test. (**f**) DNA pulldown assay. The demethylase activity of PHF2 and the ARID domain of ARID5B are required for promoter DNA binding of PHF2–ARID5B in 293F cells. Cell lysates were mixed with avidin beads which were bound to biotin-conjugated oligonucleotides bearing the indicated promoter sequence. The bound protein was detected by western blotting. There were similar levels of expression of PHF2–ARID5B and their derivatives (lower panels). Uncropped images of blots are shown in Supplementary Fig. S9.

cells[24,25]. HNF4α was enriched with PHF2–ARID5B on the promoter of *Pepck* (Fig. 6c). Knockdown of HNF4α decreased recruitment of PHF2–ARID5B to the promoters (Fig. 6c) and loss of PKA-dependent gene induction (Fig. 6d). Thus, HNF4α and FXR have emerged as transcriptional activators co-activated by PHF2–ARID5B in glucagon–PKA-induced gene expression.

Finally, the physiological relevance of the proposed PHF2–ARID5B promoter targeting was examined under fasting conditions where PKA signal was activated by glucagon in intact animals. In fasted mice, co-recruitment of PHF2 with ARID5B was detected in the promoter regions of *Pepck* and *G6Pase* in liver (Fig. 6e) with the expected decrease in H3K9Me2 modification (Fig. 6e).

DISCUSSION

Here, we have identified a PKA-dependent histone demethylase complex that conferred signal-dependent activation of its responsive genes. Assembly of the PHF2–ARID5B complex, its recruitment to target promoters, and its H3H9Me2 demethylase activity were dependent on PKA activity. Thus, the PHF2–ARID5B complex seems to serve as a signal-sensing epigenetic determinant through removal of a repressive histone methylation mark[1,2,30,31] on the transcriptionally responsive promoters. The molecular basis of signal sensing by the PHF2–ARID5B complex is attributable to PKA-phosphorylation-dependent induction of PHF2 enzymatic activity and complex assembly with the DNA-binding subunit (ARID5B). Unlike PHF2, several other jmjC demethylases possess both jmjC and ARID domains within a single molecule[3,5,8,9]. Thus, segregation of these two key domains into separate subunits may enable PHF2 enzymatic activity to be linked to PKA signalling through assembly of the PHF2–ARID5B complex and intracomplex communication. Similarly, other jmjC demethylases that are inactive as single subunits may be functionally regulated through post-translational modifications and assembly with their complex partner components. The characterization of a signal-dependent histone demethylase provides further understanding of the regulatory mechanism for dynamic epigenetic modification in physiological contexts such as energy metabolism and homeostasis. □

METHODS

Methods and any associated references are available in the online version of the paper at http://www.nature.com/naturecellbiology

Note: Supplementary Information is available on the Nature Cell Biology website

ACKNOWLEDGEMENTS

We thank D. D. Moore for critical discussion, R. Sato and J. Inoue for providing materials, N. Moriyama and S. Fujiyama for technical assistance and M. Yamaki for manuscript preparation. This work was supported in part by Priority Areas from the Ministry of Education, Culture, Sports, Science and Technology, MEXT, Japan, JSPS, and The Naito Foundation (to F.O. and S.K.).

AUTHOR CONTRIBUTIONS

A.B., F.O. and S.K. designed the study. A.B., F.O., Y.O., K.Y., M.O. and Y.I. carried out experiments. M.N., C.A.M., K.I., J.K. and M.B. carried out analyses and provided general support. F.O. and S.K. wrote the paper.

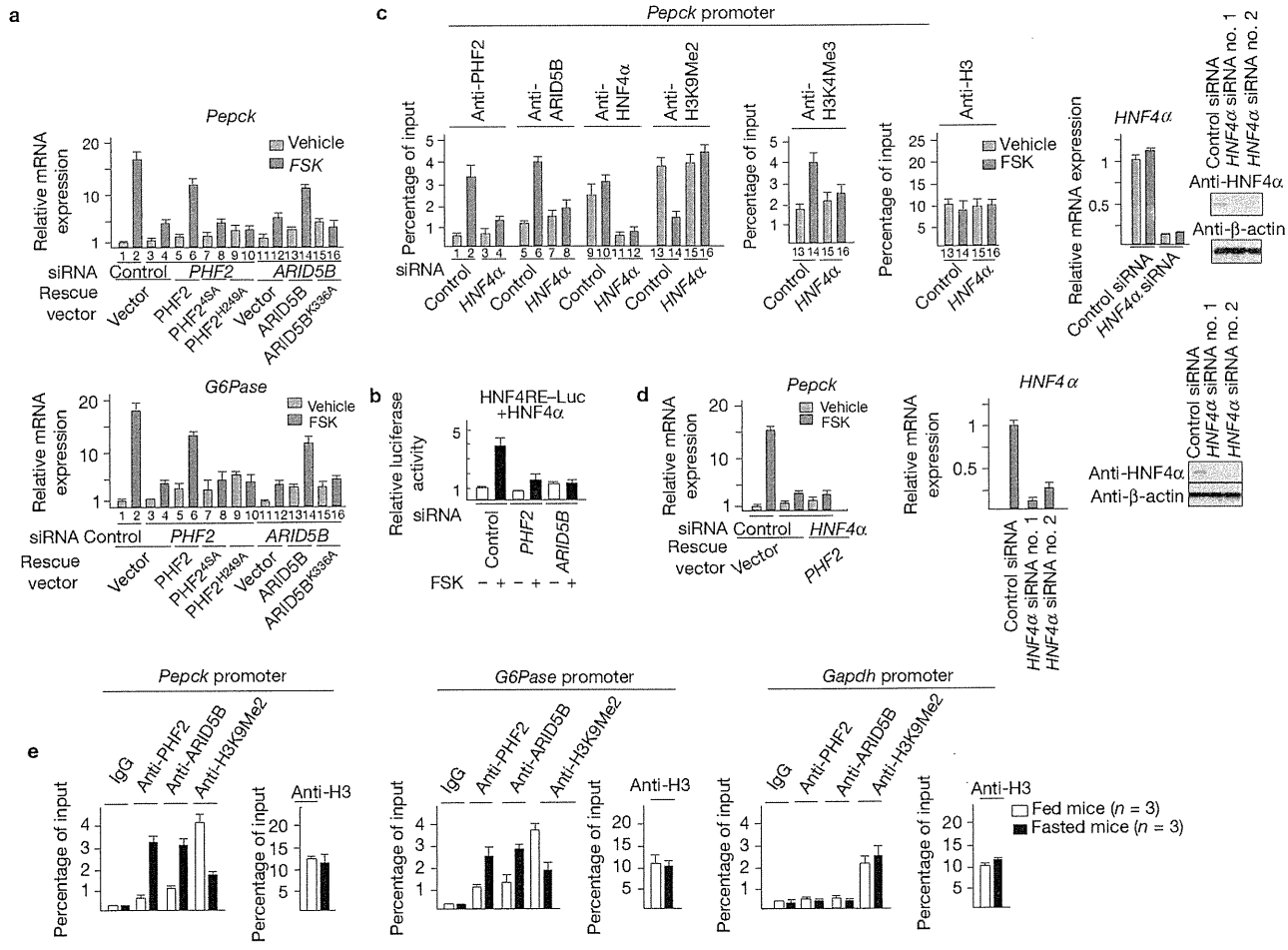

Figure 6 PHF2–ARID5B co-activates HNF4α in liver of fasted mice. (**a**) PHF2–ARID5B complex is indispensable for PKA-dependent gene induction of *Pepck* and *G6Pase*. Hepatocytes were transfected with the indicated siRNAs for 24 h, then incubated with the indicated compounds for 24 h, and quantatitive PCR with reverse transcription (RT–PCR) was carried out. Data are average ± s.d. ($n = 3$). (**b**) PHF2–ARID5B co-activates HNF4α in the presence of FSK in luciferase assays. 293F cells were transfected with the indicated plasmids in the presence or absence of FSK for 24 h. Data are average ± s.d. ($n = 3$). (**c**,**d**) Immortalized hepatocytes were transfected with HNF4α siRNA for 48 h, and ChIP assay (**c**) and quantitative RT–PCR for gene expression (**d**) were carried out. Knockdown efficiency was determined in the right panels of (**c**) and (**d**). Data are average ± s.d. ($n = 3$). (**e**) Livers from either fasted or fed mice ($n = 3$) were subjected to ChIP analyses using either anti-PHF2, anti-ARID5B, anti-H3K9Me2 or control IgG and anti-H3 antibodies. Fasting induces recruitment of PHF2–ARID5B and reduction of the H3K9Me2 mark in *Pepck* and *G6Pase* promoters, but not *Gapdh* promoter. Data shown are average ± s.d. of three independent experiments. Uncropped images of blots are shown in Supplementary Fig. S9.

COMPETING FINANCIAL INTERESTS
The authors declare no competing financial interests.

Published online at http://www.nature.com/naturecellbiology
Reprints and permissions information is available online at http://www.nature.com/reprints

1. Kouzarides, T. Chromatin modifications and their function. *Cell* **128,** 693–705 (2007).
2. Ruthenburg, A. J., Li, H., Patel, D. J. & Allis, C. D. Multivalent engagement of chromatin modifications by linked binding modules. *Nat. Rev. Mol. Cell Biol.* **8,** 983–994 (2007).
3. Iwase, S. *et al.* The X-linked mental retardation gene SMCX/JARID1C defines a family of histone H3 lysine 4 demethylases. *Cell* **128,** 1077–1088 (2007).
4. Klose, R. J., Kallin, E. M. & Zhang, Y. JmjC-domain-containing proteins and histone demethylation. *Nat. Rev. Genet.* **7,** 715–727 (2006).
5. Lee, M. G., Norman, J., Shilatifard, A. & Shiekhattar, R. Physical and functional association of a trimethyl H3K4 demethylase and Ring6a/MBLR, a polycomb-like protein. *Cell* **128,** 877–887 (2007).
6. Shi, Y. & Whetstine, J. R. Dynamic regulation of histone lysine methylation by demethylases. *Mol. Cell* **25,** 1–14 (2007).
7. Tsukada, Y. *et al.* Histone demethylation by a family of JmjC domain-containing proteins. *Nature* **439,** 811–816 (2006).
8. Christensen, J. *et al.* RBP2 belongs to a family of demethylases, specific for tri- and dimethylated lysine 4 on histone 3. *Cell* **128,** 1063–1076 (2007).
9. Klose, R. J. *et al.* The retinoblastoma binding protein RBP2 is an H3K4 demethylase. *Cell* **128,** 889–900 (2007).
10. Whetstine, J. R. *et al.* Reversal of histone lysine trimethylation by the JMJD2 family of histone demethylases. *Cell* **125,** 467–481 (2006).
11. Ohtake, F. *et al.* Dioxin receptor is a ligand-dependent E3 ubiquitin ligase. *Nature* **446,** 562–566 (2007).
12. Takada, I. *et al.* A histone lysine methyltransferase activated by non-canonical Wnt signalling suppresses PPAR-gamma transactivation. *Nat. Cell Biol.* **9,** 1273–1285 (2007).
13. Hasenpusch-Theil, K. *et al.* PHF2, a novel PHD finger gene located on human chromosome 9q22. *Mamm. Genome* **10,** 294–298 (1999).
14. Whitson, R. H., Huang, T. & Itakura, K. The novel Mrf-2 DNA-binding domain recognizes a five-base core sequence through major and minor-groove contacts. *Biochem. Biophys. Res. Commun.* **258,** 326–331 (1999).
15. Qi, H. H. *et al.* Histone H4K20/H3K9 demethylase PHF8 regulates zebrafish brain and craniofacial development. *Nature* **466,** 503–507 (2010).
16. Liu, W. *et al.* PHF8 mediates histone H4 lysine 20 demethylation events involved in cell cycle progression. *Nature* **466,** 508–512 (2010).
17. Tsukada, Y., Ishitani, T. & Nakayama, K. I. KDM7 is a dual demethylase for histone H3 Lys 9 and Lys 27 and functions in brain development. *Genes Dev.* **24,** 432–437 (2010).
18. Li, F. *et al.* Lid2 is required for coordinating H3K4 and H3K9 methylation of heterochromatin and euchromatin. *Cell* **135,** 272–283 (2008).

19. Lan, F. *et al. S. pombe* LSD1 homologs regulate heterochromatin propagation and euchromatic gene transcription. *Mol. Cell* **26,** 89–101 (2007).
20. Jiang, G. & Zhang, B. B. Glucagon and regulation of glucose metabolism. *Am. J. Physiol. Endocrinol. Metab.* **284,** E671–E678 (2003).
21. Lin, J., Handschin, C. & Spiegelman, B. M. Metabolic control through the PGC-1 family of transcription coactivators. *Cell Metab.* **1,** 361–370 (2005).
22. Mayr, B. & Montminy, M. Transcriptional regulation by the phosphorylation-dependent factor CREB. *Nat. Rev. Mol. Cell Biol.* **2,** 599–609 (2001).
23. Feige, J.N. & Auwerx, J. Transcriptional coregulators in the control of energy homeostasis. *Trends Cell Biol.* **17,** 292–301 (2007).
24. Goodwin, B. *et al.* A regulatory cascade of the nuclear receptors FXR, SHP-1, and LRH-1 represses bile acid biosynthesis. *Mol. Cell* **6,** 517–526 (2000).
25. Lu, T. T. *et al.* Molecular basis for feedback regulation of bile acid synthesis by nuclear receptors. *Mol. Cell* **6,** 507–515 (2000).
26. Koo, S. H. *et al.* The CREB coactivator TORC2 is a key regulator of fasting glucose metabolism. *Nature* **437,** 1109–1111 (2005).
27. Rhee, J. *et al.* Regulation of hepatic fasting response by PPARgamma coactivator-1α (PGC-1): requirement for hepatocyte nuclear factor 4α in gluconeogenesis. *Proc. Natl Acad. Sci. USA* **100,** 4012–4017 (2003).
28. Yoon, J. C. *et al.* Control of hepatic gluconeogenesis through the transcriptional coactivator PGC-1. *Nature* **413,** 131–138 (2001).
29. Fujiki, R. *et al.* GlcNAcylation of a histone methyltransferase in retinoic-acid-induced granulopoiesis. *Nature* **459,** 455–459 (2009).
30. Metzger, E. *et al.* LSD1 demethylates repressive histone marks to promote androgen-receptor-dependent transcription. *Nature* **437,** 436–439 (2005).
31. Rosenfeld, M. G., Lunyak, V. V. & Glass, C. K. Sensors and signals: a coactivator/corepressor/epigenetic code for integrating signal-dependent programs of transcriptional response. *Genes Dev.* **20,** 1405–1428 (2006).